

## Accepted Manuscript

A review on recent heat transfer studies to supercritical pressure water in channels

Han Wang, Laurence K.H. Leung, Weishu Wang, Qin Cheng Bi

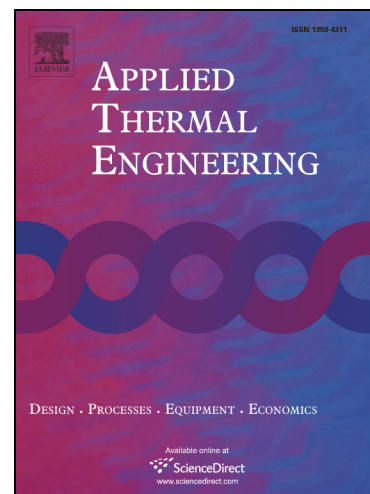
PII: S1359-4311(18)33014-X  
DOI: <https://doi.org/10.1016/j.applthermaleng.2018.07.007>  
Reference: ATE 12365

To appear in: *Applied Thermal Engineering*

Received Date: 15 May 2018  
Revised Date: 28 June 2018  
Accepted Date: 3 July 2018

Please cite this article as: H. Wang, L.K.H. Leung, W. Wang, Q. Bi, A review on recent heat transfer studies to supercritical pressure water in channels, *Applied Thermal Engineering* (2018), doi: <https://doi.org/10.1016/j.applthermaleng.2018.07.007>

This is a PDF file of an unedited manuscript that has been accepted for publication. As a service to our customers we are providing this early version of the manuscript. The manuscript will undergo copyediting, typesetting, and review of the resulting proof before it is published in its final form. Please note that during the production process errors may be discovered which could affect the content, and all legal disclaimers that apply to the journal pertain.



# A review on recent heat transfer studies to supercritical pressure water in channels

Han Wang<sup>a,b</sup>, Laurence K.H. Leung<sup>c</sup>, Weishu Wang<sup>d</sup>, Qincheng Bi<sup>e,\*</sup>

<sup>a</sup> School of Nuclear Science and Engineering, North China Electric Power University, Beijing 102206, China

<sup>b</sup> Beijing Key Laboratory of Passive Safety Technology for Nuclear Energy, North China Electric Power University, Beijing 102206, China

<sup>c</sup> Canadian Nuclear Laboratories, Chalk River, Ont. K0J1J0, Canada

<sup>d</sup> North China University of Water Resources and Electric Power, Zhengzhou 450011, China

<sup>e</sup> State Key Laboratory of Multiphase Flow in Power Engineering, Xi'an Jiaotong University, Xi'an 710049, China

## Abstract

Recent studies on heat transfer to super-critical water (SCW) in tubes, annuli and rod bundles have been reviewed in support of the development of supercritical water-cooled reactors. Experimental investigations are primarily focused on the heat transfer deterioration (HTD) to examine its general behavior, transition boundary and physical mechanisms. Large amount of experimental data were obtained from the experiments supplementing the extensive database previously compiled for fossil fuel-fired power plants. Prediction methods for heat-transfer coefficient were developed from various databases. These methods provide reasonable predictions at normal and enhanced heat-transfer regions, but fail to capture HTD. The upstream effects have not been considered in the prediction methods and may have an impact on local heat transfer, particularly in a channel with a non-uniform axial power profile or with flow/pressure transients. Most numerical studies evaluated the applicability of turbulence models to SCW using the computational fluid dynamics tools. Significant

---

\* Corresponding author. Tel.: +86 29 82665287.

E-mail addresses: [wanghan@ncepu.edu.cn](mailto:wanghan@ncepu.edu.cn) (H. Wang), [laurence.leung@cnl.ca](mailto:laurence.leung@cnl.ca) (L.K.H. Leung), [wangweishu@ncwu.edu.cn](mailto:wangweishu@ncwu.edu.cn) (W.S. Wang), [qcbi@mail.xjtu.edu.cn](mailto:qcbi@mail.xjtu.edu.cn) (Q.C. Bi).

challenges remain in establishing the reliability of the turbulence models and the modeling of buoyancy and turbulent heat flux. Direct numerical simulation and large eddy simulation have been applied in understanding the HTD phenomena. These studies are limited to simple channels over a short axial distance at relatively low Reynolds numbers.

**Keywords:** Supercritical water; heat transfer; experimental investigation; heat transfer deterioration; turbulence modeling; empirical correlation

### Nomenclature

$c_p$	specific heat [kJ/(kgK)]
$\bar{c}_p$	average specific heat [kJ/(kgK)]
$C_b, C_{t1}, C_{t2}, C_{t3}$	coefficients of AHFM model [-]
$d$	diameter [mm]
$D_{hy}$	hydraulic equivalent diameter [mm]
$f$	friction factor [-]
$f_u$	damping function [-]
$G$	mass flux [kg/m <sup>2</sup> s]
$G_k$	production of $k$ due to buoyancy [kg/(m <sup>3</sup> s <sup>3</sup> )]
$Gr$	Grashof number $\frac{(\rho_b - \rho_w) D_{hy}^3 g}{\rho \nu^2}$ [-]
$\overline{Gr}$	average Grashof number $\frac{(\rho_b - \bar{\rho}) D_{hy}^3 g}{\rho \nu^2}$ [-]
$Gr^*$	Grashof number based on heat flux $\frac{g \beta q D_{hy}^4}{\lambda \nu^2}$ [-]
$g$	gravity constant [m/s <sup>2</sup> ]
$h$	heat transfer coefficient [kW/(m <sup>2</sup> K)]
$H$	enthalpy [kJ/kg]
$k$	turbulent kinetic energy [m <sup>2</sup> /s <sup>2</sup> ]
$L$	length [m]
$M$	molecular weight [kg/kmol]
$Nu$	Nusselt number $\frac{h \cdot D_{hy}}{\lambda}$ [-]

$P$	pressure [MPa]
$Pe_t$	turbulent Peclet number $\frac{\mu_t}{\mu} Pr$ [-]
$Pr$	Prandtl number $\frac{\mu \cdot c_p}{\lambda}$ [-]
$Pr_t$	turbulent Prandtl number $\frac{\varepsilon_M}{\varepsilon_H}$ [-]
$\overline{Pr}$	average Prandtl number $\frac{\mu \cdot \overline{c_p}}{\lambda}$ [-]
$q$	heat flux [kW/m <sup>2</sup> ]
$q_t$	turbulent heat flux [m <sup>3</sup> /s <sup>3</sup> ]
$q^+$	non-dimensional heat flux $\frac{q\beta}{G c_p}$ [-]
$Re$	Reynolds number $\frac{\rho \cdot u \cdot d}{\mu}$ [-]
$t$	temperature [°C]
$\overline{t'^2}$	temperature variance [°C <sup>2</sup> ]
$T$	temperature [K] or [°C]
$u$	velocity [m/s]
$u^+$	non-dimensional velocity [-]
$x$	length from the inlet of the test section [mm]
$y^+$	non-dimensional distance from wall [-]
<i>Greek letters</i>	
$\rho$	density [kg/m <sup>3</sup> ]
$\lambda$	thermal conductivity [W/(mK)]
$\mu$	dynamic viscosity [Pa·s]
$\mu_t$	turbulent viscosity [Pa·s]
$\nu$	kinematic viscosity [m <sup>2</sup> /s]
$\varepsilon$	turbulent dissipation rate [m <sup>2</sup> /s <sup>3</sup> ]
$\omega$	specific dissipation rate [1/s]
$\phi'$	Reynolds-averaging fluctuation of $\phi$ [-]
$\beta$	thermal expansion coefficient [1/°C]
<i>Subscripts</i>	
av	average

b	bulk
cr	critical
in	inlet
pc	pseudo-critical
w	wall

## Abbreviations

AHFM	algebraic heat flux model
CFD	computational fluid dynamic
DHT	deteriorated heat transfer
DNB	departure from nucleate boiling
DNS	direct numerical simulation
GIF	Generation-IV International Forum
HTD	heat transfer deterioration
LES	large eddy simulation
P/D	pitch-to-diameter ratio
q/G	heat-flux to mass-flux ratio
R&D	research and development
RANS	Reynolds-Averaged Navier-Stokes
SCW	supercritical water
SCWR	Supercritical Water-cooled Reactor

## Content

1. Introduction.....	6
2. Thermophysical properties of supercritical water.....	7
3. Heat-transfer behaviors.....	8
4. Experimental investigations.....	10
4.1. Heat transfer in tubes, annuli and rod bundles .....	10
4.2. Influencing factors on heat transfer .....	14
4.2.1. Effects of system parameters .....	14
4.2.2. Effects of tube diameter.....	16
4.2.3. Effects of flow direction .....	17
4.2.4. Effects of flow geometry .....	18
4.2.5. Effects of upstream condition .....	19
4.3. Heat transfer deterioration.....	20
4.3.1. General behavior of HTD .....	20
4.3.2. Prediction for the onset of HTD.....	21
4.3.3. Mechanisms of HTD .....	22
4.3.4. Methods to improve heat transfer .....	25
5. Numerical simulation .....	26
5.1. Overview of recent numerical works.....	27
5.2. Modeling of heat transfer deterioration .....	29
5.3. Improvements to the modeling of turbulent heat flux .....	32
5.3.1. Variable turbulent Prandtl number.....	32
5.3.2. Algebraic Heat Flux Model .....	34
5.4. Advanced simulations of LES and DNS.....	36
6. Prediction methods.....	37
7. Conclusions.....	40

## 1. Introduction

Supercritical pressure fossil fuel-fired power plants with water as coolant have been widely adopted to improve the thermal efficiency (currently about 48%) [1, 2]. The use of supercritical pressure water (SCW) in nuclear power plants was explored in the 1960s. Since 2000, there is a renewed interest in developing the Super-Critical Water-cooled Reactor (SCWR) to improve the economic, safety, proliferation resistance and sustainability of the current generation of nuclear systems for commercialized by 2030 [3]. Several conceptual designs have been developed, including the Super-Critical Light-Water Reactor (SCLWR) and the Super-Critical Fast Reactor (SCFR) of Japan [4], High Performance Light-Water Reactor (HPLWR) of Europe [5], Canadian SCWR of Canada [6] and Super-Critical Pressure Vodo-Vodyanoi Energetichesky Reactor (VVER-SKD) of Russia [7]. A collaborative effort has been established for Research and Development (R&D) in support of the development under the Generation-IV International Forum (GIF) [8].

Raising the pressure and temperature above the thermodynamic critical point of water (374 °C, 22.1 MPa) for the SCWRs increases the thermal efficiency from about 33% of the light-water reactors to as high as 45% [9]. This would enhance the fuel utilization and minimize waste stream. Furthermore, phase change of water is not encountered during normal operation at supercritical pressures facilitating the direct transfer of coolant from the reactor outlet to the high-pressure turbine (i.e., direct cycle) eliminating the needs of steam generators (as in pressurized-water reactors) and moisture separators (as in boiling-water reactors). This simplifies considerably the nuclear steam supply system and reduces the reactor plant size and footprint, which leads to significant capital cost saving compared to the current generation of nuclear reactors [3].

Thermal-hydraulics has been identified as one of the critical knowledge areas for the SCWR development [8]. Collaborative R&D are established for heat transfer, hydraulic resistance, stability and critical flow within the GIF-SCWR System.

Extensive efforts have been devoted to understanding the heat transfer from channels to SCW, which has a strong impact on the design of core and fuel of the SCWRs.

Extensive reviews were presented on heat transfer to fluids at supercritical pressures by Cheng and Schulenberg [10], Pioro et al. [11] and Pioro and Duffey [12]. A large number of research studies on heat transfer of SCW were reported within the last decade. Recently, Rahman et al. [13] provides a literature survey on heat transfer at supercritical pressures for nuclear applications, covering both experimental studies and numerical simulations. It enhances the understanding of basic heat-transfer phenomena of SCW and is valuable to SCWR developers. Huang et al. [14] focuses on discussing the heat transfer characteristics of supercritical fluids (water, carbon dioxide and hydrocarbon fuels) in smooth channels as well as enhanced tubes. Phenomena such as heat transfer deterioration and wire-wrapped spacers on heat transfer were studied. While it is essential for engineering applications, it fails to cover the heat transfer of SCW in rod bundles which are more relevant to the fuel assembly of SCWR. Therefore, it is the objective of this paper to present the latest review of experimental and numerical findings related to heat transfer at supercritical pressures in tubes, annuli and rod bundles. It may serve as a necessary supplement to the above-mentioned review studies. In view of the relevancy to SCWR development, this review focuses on heat transfer to water even though significant efforts have been devoted to the use of surrogate fluids (such as carbon dioxide and refrigerants) as coolant in experiments.

## **2. Thermophysical properties of supercritical water**

Thermophysical and transport properties of SCW undergo sharp and non-linear variations at the vicinity of the pseudo-critical temperature. Fig. 1 shows the phases of water in the pressure-temperature diagram established from the NIST-REFPROP database [15]. At a given subcritical pressure, the temperature of liquid water increases until the saturation point, where the water vaporizes to steam (vapor). Continuously increasing the steam temperature would categorize as superheated vapor (or steam). As indicated in the figure, the saturated-temperature point is unique at

each pressure and increases with increasing pressure. For pressures beyond the critical point, the phase change from liquid to vapor is not encountered. Instead, fluid properties vary gradually with increasing temperature until reaching the pseudo-critical point where a sharp variation is encountered.

(Insert Figure 1)

Fig. 2 shows the variation of thermophysical properties of SCW with temperature at various pressures. As shown in Fig. 2(a), the specific heat increases gradually at the liquid-like region and decreases at the vapor-like region with increasing temperature. It occurs a “Λ-shaped” profile at the transition. The temperature corresponding to the maximum value of the specific heat is referred to as the pseudo-critical temperature, which increases with pressure. The peak of specific heat, on the other hand, decreases with increasing pressure. Fig. 2 (b) shows the variation of density with temperature. The density decreases with increasing temperature; the reduction is relatively rapid at the vicinity of the pseudo-critical temperature as the liquid-like fluid changes to vapor-like fluid. The rapid reduction at the pseudo-critical temperature becomes less pronounced at high pressures. Similar variations to the density are shown for the dynamic viscosity in Fig. 2(c) and for the thermal conductivity in Fig. 2(d). However, a local peak in the thermal conductivity exhibits as the temperature approaches the pseudo-critical point. It diminishes with increasing pressure.

(Insert Figure 2)

### **3. Heat-transfer behaviors**

As indicated previously, phase change of water is eliminated with increasing temperature at supercritical pressures. Therefore, current safety criteria for nuclear reactor operation, based on the departure from nucleate boiling (DNB) or dryout, are no longer applicable [8]. Instead, developers of the SCWR concepts have adopted the peak cladding and fuel centre-line temperatures as the criteria. This would require

improved understanding of the heat-transfer phenomena at supercritical pressures and accurate prediction methods for heat-transfer coefficients.

In view of the lack of phase change, water at supercritical pressures is considered a single-phase fluid with associated single-phase heat transfer characteristics in a heated channel. These characteristics can be represented with a single-phase heat-transfer correlation, such as the Dittus and Boelter [16] correlation which is expressed as:

$$Nu_b = 0.023Re_b^{0.8}Pr_b^{\frac{1}{3}} \quad (1)$$

However, the sharp variations in the thermophysical properties at the vicinity of the pseudo-critical point challenge the application of this heat transfer correlation. In addition, the complex buoyancy and acceleration effects at the near-wall region have led to significant changes to the single-phase heat-transfer characteristics. Fig. 3 presents the ratios of the experimental heat transfer coefficient,  $h$ , to the prediction using the Dittus-Boelter [16] correlation,  $h_0$ , with bulk-fluid temperature at various heat fluxes in a vertical heated tube. At the heat flux of  $200 \text{ kW/m}^2$ , the ratio of heat-transfer coefficient is smaller than 1 at the bulk-fluid temperature of 550 K and increases gradually with bulk temperature to a local maximum at the vicinity of the pseudo-critical point (658 K). It decreases sharply at the pseudo-critical point, beyond which the reduction becomes gradual and approaches the value of 1 with increasing bulk-fluid temperature. The peak in heat-transfer-coefficient ratio has been identified as the heat transfer enhancement. However, the identification is mainly attributed to the predicted trend in heat-transfer coefficient using the Dittus-Boelter [16] correlation, as shown by the green line in Fig. 3.

(Insert Figure 3)

The peak ratio of heat-transfer coefficient becomes lower and shift to low temperature with increasing heat flux. On the other hand, the drop in heat-transfer ratio is more severe and forms a valley near the pseudo-critical temperature. The peak and valley in heat-transfer ratio may occur at the same heat flux, which indicates a

transition in the heat transfer mechanisms. As described by Cheng and Liu [17], R&D efforts focused on the understanding of these behaviors.

Before proceeding to the next section, some definitions related to the heat transfer at supercritical pressures need to be clarified. The pseudo-critical temperature region refers to the temperature range of  $\pm 25$  °C around the pseudo-critical temperature, where the thermophysical properties vary sharply [18]. The corresponding range of enthalpy is referred to as the pseudo-critical enthalpy region. Normal heat transfer refers to the heat transfer coefficients similar to those predicted using the Dittus-Boelter [16] correlation in regions far from the pseudo-critical enthalpy region. Enhanced heat transfer is characterized by an increase in heat transfer coefficient beyond the prediction of the Dittus-Boelter [16] correlation (i.e.,  $h/h_0 > 1$ ). Deteriorated heat transfer (DHT), or heat transfer deterioration (HTD), is characterized by the rapid increase in the wall temperature or the drop in the heat transfer coefficient compared to normal heat transfer. Unlike the features of DNB, it is difficult to identify the onset of HTD due to the relatively gradual increase in the wall temperature. Heat-transfer ratio less than 0.3 (i.e.,  $h/h_0 < 0.3$ ) is often considered as the occurrence of HTD [11, 19, 20].

## 4. Experimental investigations

### 4.1. Heat transfer in tubes, annuli and rod bundles

The investigation on heat transfer of SCW originated from the 1950s driven by the need of developing supercritical fossil fuel-fired power plants. Up to now, more than 200 experimental papers have been published, most of which were reviewed in Piro and Duffey [21]. Earlier studies, such as Shitsman [22], Bishop et al. [23], Swenson et al. [24] and Yamagata et al. [19], focused on experiments with SCW flowing inside tubes. These studies showed that the heat transfer is enhanced when the bulk temperature is below while the wall temperature is above the pseudo-critical temperature. The enhancement diminishes gradually with increasing heat flux. DHT occurs at relatively low mass fluxes or high heat fluxes with a rapid increase in the wall temperature. It has been observed at locations near the inlet of the test section or

close to the pseudo-critical temperature. Heat-transfer data obtained from these experiments have been applied in benchmarking or validating computational fluid dynamics (CFD) tools and models.

Despite of the availability of experimental heat transfer data at supercritical pressures, additional heat-transfer experiments with SCW are still required because (i) the physical mechanisms of the DHT phenomena are still not fully understood, (ii) about half of the heat-transfer data of SCW are no longer available, especially those obtained prior to 1965 [25]; (iii) available data have an uncertainty of 15% or more, due to the discrepancy in thermophysical properties adopted in the analyses and in calculating methods for wall temperature [26]. Table 1 lists the heat-transfer experiments with SCW in tubes performed after 2005.

(Insert Table 1)

As shown in Table 1, recent heat-transfer experiments of SCW in smooth tubes covered the pressures from 11 to 32 MPa, mass fluxes from 170 to 2200 kg/m<sup>2</sup>s, heat fluxes up to 3210 kW/m<sup>2</sup> and tube diameters from 6.28 to 43 mm. Those with large diameter tubes (i.e., Yin et al. [32], Zhu et al. [33], Yu et al. [36, 37] and Lei et al. [45]) were performed mainly for understanding the heat transfer of SCW in water-walls of the supercritical boilers. Other experiments using small-diameter tubes ranging from 6.28 to 7.6 mm (i.e., Pis'menny et al. [29, 30], Zhao et al. [41] and Gu et al. [43]) are more relevant for fuel-assembly development of SCWRs, although this range of diameter is still beyond the subchannel sizes in most SCWR fuel-assembly concepts [47]. Kirillov and Grabezhnaya [26] and Mokry et al. [34, 35] focused on expanding the heat-transfer database to improve the heat-transfer correlation in support of the thermal design of SCWR fuel assembly. Experiments of Zhao et al. [41] and Gu et al. [43] covered the relevant range of conditions for SCWR development. Data from these experiments are applicable in quantifying the effects of tube diameter and flow direction on heat transfer.

Experiments with horizontal flow are of less interest for fuel assembly analyses but could be applied in piping analyses. These experiments showed non-uniform

wall-temperature distributions around the tube circumference, where a higher wall temperature was observed at the top than at the bottom portion of the tube. It is attributed to the buoyancy effect leading to a drastic drop in density within the boundary layer. The temperature difference between the top and bottom regions becomes pronounced with increasing heat flux or decreasing mass flux.

Experimental data obtained with simple tubes are not directly relevant in fuel-assembly analyses. This is attributed to the geometry difference in heated surface (i.e., concave shape in tubes compared to convex shape in fuel rods), the presence of spacing devices, gap effect, flow and enthalpy imbalances, etc. Nevertheless, tube-data-based correlations have been applied in system codes [48, 49], sub-channel codes [50] as well as CFD tools [51] for the preliminary design and analysis of fuel assemblies. Verification and validation of these tools against experimental data are required with bundle subassemblies at relevant conditions. Heat transfer experiments with SCW flowing through bundles are scarce due mainly to the lack of supercritical-pressure test loops, technical difficulties in test-section construction, high operating cost and extensive operating duration [10, 52]. Pioro and Duffey [12] reviewed that, as of 2004, the majority of experiments were performed with tubes and only two studies (Dyadyakin and Popov [53] and Silin et al. [54]) were carried out using bundles. In the last decade, several experimental studies on heat transfer to SCW were performed with test sections other than tubes, generating a large amount of data points in support of developing SCWRs. These recent studies are summarized in Table 2.

(Insert Table 2)

Licht et al. [55] performed heat transfer experiments with SCW in two annuli (one with a circular shroud and the other with a square shroud). They observed a notable effect of channel geometry on HTD. In a subsequent experiment [74], the mean and turbulent velocities were measured using a two-component laser Doppler velocimetry system to understand the phenomena of heat transfer enhancement and

deterioration. These measurements were applied for validating and improving turbulence models in CFD tools.

Razumovskiy et al. [58-60] conducted heat transfer experiments with SCW in an annulus channel, a 3-rod bundle and a 7-rod bundle. Spacings between the heated rods and the unheated shroud were tight in these channel configurations. DHT was observed in these experiments at high heat fluxes.

Li et al. [61] and Gang et al. [62] performed experiments using annular flow channels with various gap sizes and channel shapes. Wire-wrapped spacers were installed along the heated rods. Assessments of several tube-data-based correlations showed a good prediction accuracy for the Jackson correlation [44], as observed in Licht et al. [55]. Yang et al. [63] conducted experiments with both upward and downward flows inside an annular channel with a gap size of 2 mm and a heated length of 620 mm. The effects of grid spacer and flow direction on heat transfer in forced and mixed convections were quantified.

Li et al. [64] observed two types of HTD in an annular channel with grid spacers. The occurrence of HTDs was attributed to buoyancy and thermal acceleration. Zhao et al. [73] examined the effect of grid spacer on heat transfer in an annular channel. Heat transfer enhancement is strong near the spacer but diminishes exponentially with increased distance downstream from the spacer. A correlation was derived in predicting the local heat-transfer enhancement due to the spacer.

Heat transfer experiments using a 2×2 rod bundle were carried out by Wang et al. [66, 71]. A fuel-assembly simulator (Pitch-to-Diameter,  $P/D=1.18$ ) with four heated rods was installed inside a square channel with rounded corners. The outer diameter of each heated rod is 8 mm and the effective heated length is 600 mm. The study was separated into two phases. The first phase focused on analyzing the heat transfer of SCW in a bare-rod bundle whereas wire-wrapped spacers were installed on the heated rod in the second phase. Non-uniform wall-temperature distributions were observed around the heated rods in the bare-rod bundle. As shown in Fig. 4(a), the maximum wall temperature was detected in the corner sub-channel while the minimum in the central sub-channel. For the wire-wrapped bundle, the

circumferential distribution in the wall temperature becomes more complex due not only to the non-uniform flow area, but also the presence of the wrapped wires. The average heat transfer in the wire-wrapped rod bundle is better than that in the bare-rod bundle. Jackson correlation [44] was found to be effective in predicting the heat transfer coefficients.

Similar experiments were performed by Gu et al. [67, 68, 70] using a 2×2 rod bundle with a rod diameter of 10 mm and heated lengths of 833 and 750 mm. The flow channel, however, was divided into two sections. Water flowed downward in the outer section to the bottom of the channel and reversed direction flowing upward in the inner section where the heated rods are located. For the bare-rod bundle, the wall temperatures along the circumference of the rod are non-uniform, as shown in Fig. 4(b). The profiles are similar to those observed by Wang et al. [66]. DHT was observed in the wire-wrapped rod bundle, the spacers appeared to suppress, but not eliminate, the occurrence of HTD. The correlations of Bishop et al. [23] and Jackson and Fewster [69] provided accurate predictions in the heat transfer coefficient.

(Insert Figure 4)

## 4.2. Influencing factors on heat transfer

Significant effects of the enthalpy, heat flux, mass flux, pressure, flow area, flow direction, channel geometry, spacing devices and upstream flow conditions have been observed on heat transfer at supercritical pressures. Ample experimental data and information were obtained. Selected studies are presented below.

### 4.2.1. Effects of system parameters

Similar observations were noted in tubes [19, 24, 40, 75], annuli [55, 61, 62] and rod bundles [66-68, 71]. Normal and enhanced heat transfer were observed at low heat fluxes where the heat transfer coefficient increases gradually with bulk enthalpy at the liquid-like region but rather rapidly at the vicinity of the pseudo-critical enthalpy. The trend reverses at the vapor-like region with high bulk enthalpy. This has resulted in a peak in the heat transfer coefficient near the pseudo-critical point. The peak reduces in magnitude and shifts to the low-enthalpy region with increasing heat

flux. However, little changes in the heat transfer coefficient with heat flux were found at the low- and high-enthalpy regions beyond the vicinity of the pseudo-critical point. Effectiveness of heat transfer reduces with increasing heat flux and the peak of heat transfer coefficient diminishes gradually. At high heat fluxes, HTD, which is characterized by a rapid drop in the heat transfer coefficient, could be encountered at liquid-like fluid conditions near the pseudo-critical point. The heat transfer coefficient recovers gradually beyond the HTD point. This phenomenon was detected by Gang et al. [62], Yang et al. [63], Wang et al. [66, 71] and Gu et al. [67, 68]. The transition from enhanced heat transfer to DHT with increasing heat flux was reported in Shitsman [22] and Li et al. [61].

For forced convective flows, the heat transfer coefficient usually increases with increasing mass flux. HTD was observed by Gang et al. [62] in their experiment with a 6-mm gap annulus at the pressure of 25 MPa, heat flux of  $600 \text{ kW/m}^2$  and mass flux of  $350 \text{ kg/m}^2\text{s}$ . As the mass flux was increased from 350 to  $690 \text{ kg/m}^2\text{s}$ , HTD was not encountered and an enhancement occurred at the vicinity of the pseudo-critical enthalpy. The heat transfer was further improved when the mass flux was increased to  $1010 \text{ kg/m}^2\text{s}$ . Similar trends have been found in other researches [33, 61, 68]. The heat-transfer enhancement was attributed to the increase in turbulent intensity at high mass fluxes (or large Reynolds numbers). The heat-transfer enhancement with increasing mass flux is systematic over the entire bulk enthalpy region. However, it is more pronounced at low than high mass fluxes [66]. Zhao et al. [41] observed a heat-transfer enhancement at the low-enthalpy region for downward flow in a smooth tube. However, the enhancement diminished in the pseudo-critical region, which could be attributed to heat-transfer deterioration.

The effect of pressure on heat transfer at supercritical pressures varies with heat transfer regimes. At a relatively small  $q/G$ , normal and enhanced heat transfer have been observed. Wang et al. [66] and Gu et al. [67, 68] showed that the heat transfer coefficient is not affected by pressure at low- and high-enthalpy regions, but increases with reduced pressure at the pseudo-critical enthalpy region. Furthermore, heat transfer is enhanced as the pressure approaches the critical point (22.1 MPa for

water). Since the variation in the heat transfer coefficient resembles the profiles of the specific heat at various pressures, many researchers [33, 62, 76] believe that the heat transfer enhancements occurring in the pseudo-critical region are mainly attributed to the drastic rise in specific heat. As the fluid temperature within the boundary layer approaches the pseudo-critical temperature, a sharp increase in the specific heat would mean the fluid is capable of absorbing heat with a relatively minor increase in wall temperature. Thus, the heat transfer is enhanced around the pseudo-critical temperature. At a relatively large ratio of  $q/G$ , DHT may occur and the effect of pressure on heat transfer coefficient appears reversing. Li et al. [61] and Gang et al. [62] demonstrated that HTD at 23 MPa occurs earlier and is more severe than that at 25 MPa under the same heat flux and mass flux conditions. Wang et al. [77] experimentally and numerically studied the HTD at low mass fluxes in an annular channel. Under the same mass flux and heat flux, HTD in the downward flow occurred at 23 MPa, but was absent at 25 MPa.

#### 4.2.2. Effects of tube diameter

Dittus-Boelter [16] correlation shows that the single-phase heat transfer coefficient is inversely proportional to the diameter (i.e.,  $h \propto d^{-0.2}$ ) at a constant mass flux. This relationship is generally valid for normal and enhanced heat transfer at relatively large mass fluxes where buoyancy effect is negligible [37, 78-80]. The look-up table developed by Loewenberg et al. [81] also supports this relationship between the heat transfer coefficient and tube diameter. Gang et al. [62] observed a strong diameter effect at a small  $q/G$  for water flow in annuli of two different gap sizes. Gu et al. [43] reported a slightly higher heat transfer coefficient for a large-diameter tube at the low-enthalpy region, but the trend reverses at the pseudo-critical region.

Buoyancy forces become strong at high heat fluxes or low mass fluxes, and may lead to the occurrence of HTD. Several studies [79, 82, 83] showed that buoyancy is weakened in small-diameter tubes. Bae et al. [84] reported a slightly higher heat transfer coefficient in large-diameter than small-diameter tubes with carbon dioxide when HTD occurs. Yamashita et al. [78] observed that the heat transfer coefficients

are independent of tube diameter in the case of HTD. Yildiz and Groeneveld [85] concluded that heat flux is the dominant factor determining the effect of tube diameter on heat transfer. In addition, this effect varies with the heat-transfer regime, degree of buoyancy, flow geometry and bulk-enthalpy range. Further studies are required to quantify the effect of tube diameter on heat transfer at supercritical pressures.

#### 4.2.3. Effects of flow direction

The effect of flow direction on heat transfer depends largely on the magnitude of buoyancy. The direction of buoyancy is always vertically upward, which aids the upward flow in tubes but opposes the downward flow [86]. For horizontal tubes, buoyancy is perpendicular to the flow direction, and may introduce a strong secondary flow on the cross-section impacting the heat transfer. Early study of Shiralkar and Griffith [83] showed that the wall temperatures in upward and downward flows are almost identical even at low mass fluxes, indicating that the flow direction has a negligible effect on heat transfer. Yamagata et al. [19] found that, the wall temperatures are almost identical for vertically upward and horizontal tubes at low heat fluxes. With the increase of heat flux, the wall temperature at the top of the horizontal tube is higher than that at the bottom, while the wall temperature of the vertically upward tube lies in between. Similar findings were also reported by Yu et al. [37] and Lei et al. [45]. They concluded that the circumferential wall temperatures of a horizontal tube are nearly overlapped in normal and enhanced heat-transfer regimes, but show a large discrepancy when DHT occurs.

Yang et al. [63] compared the heat transfer of SCW in an annulus with vertically upward and downward flows. They found that downward flow shows a superior heat-transfer performance to upward flow, and this phenomenon becomes more pronounced with increasing  $q/G$ . Wang et al. [77] further confirmed this conclusion by the fact that DHT was observed in the upward flow but did not appear in the downward flow at the same experimental parameters. Zhao et al. [41] compared the heat transfer coefficients of SCW at three heat fluxes. At low heat fluxes of 520-570  $\text{kW/m}^2$ , the heat transfer coefficient in the upward flow is 50% higher than that in the downward flow. Nevertheless, heat transfer is slightly improved in downward flow at

medium- and high heat fluxes. The experimental results of Shen et al. [40] indicated that the effect of flow direction is inconsistent within the entire bulk-enthalpy range. Lower wall temperatures were observed in an upward flow at the pseudo-critical region compared to that in a downward flow, but the trend reverses in the high-enthalpy region.

From the above-mentioned analyses, the effect of flow direction on heat transfer is complex and depends strongly on buoyancy. With increasing heat flux (or  $q/G$ ), heat transfer is more effective in the downward flow compared to the upward flow. Heat transfer effectiveness in vertical and horizontal flows is difficult to quantify due to the enthalpy imbalance at the top and bottom surfaces of a horizontal tube leading to a temperature gradient. Additional studies are needed to quantify this effect on heat transfer and confirm the findings of Shiralkar and Griffith [83], Shen et al. [40] and Zhao et al. [41].

#### 4.2.4. Effects of flow geometry

Direct comparisons of the wall temperature obtained in different flow geometries are limited in literature. DHT was detected in a tube rather than in a rod bundle under similar conditions (cross-sectional average values for the rod bundle) [54]. This seems to signify an improvement in heat transfer for the rod bundle. Jackson [87] observed that the magnitude of buoyancy-induced HTD is weakened in annuli compared to tubes. Licht et al. [55] and Li et al. [61] also reported an increase in the heat transfer coefficient for annuli compared to tubes at similar flow conditions. Zhao et al. [73] experimentally investigated the heat transfer of SCW in an annular channel. Unlike the findings of Jackson [87], Licht et al. [55] and Li et al. [61], they stated that the heat transfer coefficient of the annular channel is 10%-20% lower than that of the tube in the pseudo-critical region, although the basic trends are similar. Li et al. [64] performed a series of heat-transfer experiments in tubes, annuli and rod bundles using SCW as the testing medium. Detailed comparisons showed that the heat transfer in annuli is the poorest among the three channels, while the flow and heat transfer behaviors are more stable and enhanced in the  $2\times 2$  rod bundle. In addition, DHT occurred in the rod bundle with a  $P/D$  of 1.18 but was eliminated when the  $P/D$  was

increased to 1.3, suggesting that large-scale bundles are more favorable to improve heat transfer of SCW. The optimum  $P/D$  of the rod bundle was not provided, but a value of 1.25 was recommended by Shang [88] considering the effect of flow direction and the maximum cladding temperature.

It may be concluded that for vertically upward flow at similar experimental and geometrical conditions, the average heat transfer in a rod bundle is the most effective compared to tubes and annuli. However, it is inconclusive between tubes and annuli, whereas the experimental observations are contradicting. It is worth noting that the CFD analysis of Liu et al. [89] showed an improved heat transfer coefficient in the annular channel. Further validation of these predictions is required.

#### 4.2.5. Effects of upstream condition

Swenson et al. [24] examined the variation of heat transfer coefficient along the tube length at two inlet temperatures. They found that the heat transfer coefficients decrease in the entrance half of the test section but increase in the exit half. They concluded that the thermal-entrance effect is much more pronounced for supercritical fluids due to the severe change in the thermophysical properties. A minimal length of 56 times of  $D_{hy}$  is needed to eliminate this effect. Similar trend in the heat transfer coefficient was observed in the experiment of Gu et al. [43]. They found that both the minimum and maximum heat transfer coefficients shift to the high-temperature direction with the increase of inlet temperature, indicating that the entrance effect could exist over a much longer region than expected. Gupta et al. [18] developed a heat transfer correlation which shows a  $\pm 15\%$  error in predicting the wall temperature. The error was reduced to  $\pm 10\%$  after adding a term of  $\left(1 + e^{\frac{x}{1.5d}}\right)^{0.608}$  to account for the entrance effect. As pointed by Piro and Duffey [12], it is important to perform the heat transfer experiments of SCW using sufficiently long test sections to minimize the entrance effect.

Recently, Cheng and Liu [17] compared respectively the experimental heat transfer coefficients of SCW,  $\text{CO}_2$  and R134a in circular tubes obtained from Shanghai Jiao Tong University, Karlsruhe Institute of Technology and University of

Ottawa. Large deviations exist in the experimental data from different sources. They believed that this phenomenon is partly attributed to the upstream effect of the flow. Due to the strong variation in the thermophysical properties, a full development of the hydraulic and thermal boundary near the heated wall did not occur. The entrance effect on heat transfer cannot be neglected for supercritical fluids and should be taken into consideration when developing heat-transfer correlations.

### **4.3. Heat transfer deterioration**

#### **4.3.1. General behavior of HTD**

The phenomenon of HTD was first reported by Shitsman [22] in a heat-transfer experiment using a vertically upward tube. With the increase of heat flux, the heat transfer effectiveness is gradually weakened until HTD appears. In addition, HTD occurs initially near the outlet of the test section, and moves towards the inlet as the heat flux increased. This behavior was also reported in subsequent investigations [19, 24, 82, 83]. Two types of HTD exist at supercritical pressures. The first type occurs at low mass fluxes and high heat fluxes when the bulk temperature is far below the pseudo-critical temperature [21]. This type of deterioration usually appears in the entrance region of the test section and is mainly caused by buoyancy. The second type occurs when the bulk temperature approaches the pseudo-critical temperature and may appear at any part of the channel [21, 64]. Thermal acceleration is believed to be responsible for this type of deterioration. Another feature is that the increase in the wall temperature is a gradual process with certain limits when HTD occurs at supercritical pressures, rather than the sharp soar as DNB takes place at subcritical pressures [19].

Fig. 5 shows the variations of the wall temperature with bulk enthalpy at DHT conditions [90]. Data were collected from Shitsman's [22] experiments consisting of vertically upward flows, as well as Domin's [91] with horizontal flows. Varying mass fluxes were studied in both cases. It is seen that for the vertical tube, DHT shows a local peak within a narrow region in the bulk enthalpy. With the increase of heat flux, the peak becomes higher and shifts to the low-enthalpy direction. In addition, the

onset of HTD becomes earlier at the higher heat flux of  $340 \text{ kW/m}^2$ . For the horizontal tube, the increase in the wall temperature is not that fast compared to the vertical tube. A peaky wall temperature is still observed, but it covers a much broader range in the bulk enthalpy. Similar behaviors were reproduced in the modern experiments of Yu et al. [36] and Lei et al. [45].

(Insert Figure 5)

#### 4.3.2. Prediction for the onset of HTD

HTD should be avoided in the design and operation of SCWRs, otherwise the rapid increase in the wall temperature may overheat the fuel cladding and thus cause a failure of the fuel elements. Therefore, a thorough knowledge about the heat flux beyond which DHT occurs is desirable. Great efforts have been made to correlate the critical heat flux that determines the onset of HTD with mass flux, as summarized in Table 3. It is seen that the expression of these formulas varies significantly. Some correlations reflect simple relationships between heat flux and mass flux, such as Styrikovich et al. [92] and Vikhrev et al. [93]. Other correlations (e.g. Protopopov et al. [97] and Jackson and Hall [38]) incorporate the local thermal properties determined by the wall temperature which is further implicitly determined by heat flux. Thus, iterations are needed in using this kind of correlation which makes them inapplicable without an accurate knowledge of the heat transfer coefficient. A relatively simple correlation containing just the global parameters (i.e. heat flux, mass flux, pressure and tube diameter) is more favorable in the pre-design of SCWRs [99].

(Insert Table 3)

Although a large amount of data has been accumulated toward understanding HTD, assessments to the empirical correlations are not straightforward. The reason for this issue is that most publications focused on analyzing the behavior of HTD, rather than the onset point of HTD. Thus, the heat flux corresponding to the reported deterioration may already be beyond the critical value. In order to assess the predictions, such case should be excluded from the database. Schatte et al. [99]

collected 4455 heat-transfer data points of SCW in vertically upward tubes from 14 independent sources. 451 data relevant to HTD were screened based on the definition of  $h/h_0 < 0.3$ , which falls within 44 independent combinations of the experimental parameters. Within these combinations, 12 cases were further removed because the heat flux was not reported as the critical one to cause the onset of HTD. Fig. 6 plots the critical heat flux predicted by selected correlations from Table 3 against the remaining data points of Schatte et al. [99] (with  $\pm 15\%$  error bars) at a pressure of 25 MPa and a tube diameter of 10 mm. It is seen that the correlations of Petukhov et al. [31] and Li et al. [98] significantly overestimate the critical heat flux. Most of the experimental data fall between the lower boundary of Vikhrev et al. [93] and the upper boundary of Ogata and Sato [96]. The comparison shows that the predictions given by Lokshin et al. [94] and Mokry et al. [35] lie in the middle of the two boundaries, indicating that these two correlations may be used for preliminary estimations. It should be emphasized that HTD depends strongly on the flow geometry, and extrapolating the conclusions to a geometry other than tubes may be invalid. In fact, some heat-flux points in Fig. 6 are not high enough to trigger a deterioration in annuli and rod bundle [62, 63, 66, 71, 77]. In other words, the optimal correlations for circular tube are usually conservative. To predict the onset of HTD in annuli and rod bundles, the correlations of Cheng et al. [42] and Schatte et al. [99] are recommended.

(Insert Figure 6)

#### 4.3.3. Mechanisms of HTD

In spite of the huge amount of experimental and numerical studies, debates still exist on the mechanisms of HTD owing to the complex variable-property flow at supercritical pressures. In literature, there are several viewpoints to explain the occurrence of HTD. Goldmann [102] and Ackerman [82] believed that HTD at supercritical pressures resembles the feature of DNB. They assumed that HTD is caused by the transition from pseudo-nucleate to pseudo-film boiling. In this process, the low-density fluid near the wall blocks the motion of high-density fluid from the

core in rewetting the wall, which is similar to the behaviors of the bubble and liquid causing DNB [76]. With the increase of heat flux, the pseudo-nucleate boiling becomes the controlling phenomenon, and finally transits into pseudo-film boiling and leads to the deterioration in heat transfer. Nevertheless, this two-phase fluid-dynamic-based theory is not widely accepted [24, 76, 103].

A growing number of studies [20, 38, 74, 76, 87, 104, 105] indicated that the drastic variations in the thermophysical properties near the pseudo-critical point and the consequent effects of buoyancy and thermal acceleration are the main reasons for HTD. Buoyancy is caused by the difference in the radial density between the boundary layer and the core, and is especially pronounced at low mass fluxes. As the wall temperature exceeds the pseudo-critical temperature, a sharp drop in the fluid density occurs in the boundary layer. With the aid of gravity, this thin layer of “light fluid” rises quickly and distorts the forced-convective velocity profile. For a vertically-upward flow, the velocity gradient becomes flattened which suppresses the turbulent production. The reduction in turbulent kinetic energy near the wall impairs the turbulent heat and momentum diffusions and finally leads to HTD. For a vertically-downward flow, buoyancy is in the opposite direction to the flow, which results into a steeper velocity gradient. Thus, heat transfer is supposed to be improved in a downward flow. The theory of buoyancy-induced relaminarization is supported by the experimental findings that HTD occurs in the upward flow but is absent in the downward flow under the same conditions [30, 38, 77, 106].

At high mass fluxes, HTD might still occur regardless of the flow direction. In this case, the effect of buoyancy is negligible due to the strong inertia force, and HTD is mainly caused by thermal acceleration. In a heated channel with a constant flow area, the bulk temperature increases from the inlet to the outlet. As can be expected, the bulk density decreases accordingly. Since the mass flux is constant at any part of the channel, the fluid accelerates as a consequence of the reduction in density. However, the velocity in the boundary layer is lower than that in the bulk flow due to the non-sliding condition attached to the wall. The shear stress in the buffer layer becomes smaller than that in a flow without acceleration. Thus, turbulence and heat

diffusion are reduced, both of which result into the deterioration. The theory of thermally-induced acceleration is upheld by investigators such as Jackson [86], Wang et al. [76], Palko and Anglart [104, 107], Zhang et al. [106], Wen and Gu [108] and Mohseni and Bazargan [109].

Apart from the buoyancy and thermal acceleration that stem directly from the drastic change in the fluid density, the variation of other properties also plays an important role to the occurrence of HTD. The temperature in the thin boundary layer increases with the wall temperature, and once it surpasses the pseudo-critical point, the peak of the specific heat moves away from the wall. Consequently, the heat-removable condition of the wall reduces further. Another important factor is the sudden drop in the thermal conductivity at the vicinity of the pseudo-critical temperature. Heat transfer from the wall to the boundary layer is greatly impaired due to the decline in the thermal conductivity. Mohseni and Bazargan [109] argued that this is the most important factor causing HTD at high mass fluxes. Furthermore, the drop in the dynamic viscosity reduces the shear stress between the near-wall layer and the core flow. As a consequence, the flow regime in the boundary layer may transform from turbulent to laminar. The combination of these unfavorable effects contributes to the occurrence of HTD.

Recently, Mohseni and Bazargan [110] proposed another theory to clarify the mechanisms of HTD. They believed that some available data of HTD could be better explained by the variation of turbulent viscosity. An increase in the wall temperature reduces the near-wall fluid density, which causes a reduction in the turbulent viscosity ( $\mu_t = \rho f_u k^2 / \varepsilon$ ). According to the equations of turbulent kinetic energy ( $k$ ) and its dissipation rate ( $\varepsilon$ ), both the turbulent diffusion term and production term decline as a result of the reduced turbulent viscosity. Therefore, the turbulent thermal diffusion is less effective and the turbulent kinetic energy is lowered, impairing heat transfer, causing a higher wall temperature and subsequently a lower turbulent viscosity. In a closed system, the heat transfer is impaired and eventually transforms into deterioration. This explanation could be further supported by the fact that the peak in the wall temperature disappeared once the turbulent viscosity was set to a constant

value in their CFD codes. The starting point of the explanation is the set of mathematical equations which define the relationships between the turbulent variables and the thermophysical properties. This viewpoint is relatively new and needs to be validated by more experimental data as well as advanced simulations.

As stated above, buoyancy-induced relaminarization, thermally-induced acceleration and the variation of turbulent viscosity are existing explanations to the mechanisms of HTD. All of the three viewpoints originate from the drastic variation in the thermophysical property near the pseudo-critical temperature, especially the density. In addition, all three theories attribute the occurrence of HTD to the decrease in turbulence near the heated wall. The direct influence of the thermophysical properties on heat transfer should never be ignored, because this is the origin of the unusual heat transfer phenomena occurred at supercritical pressures.

#### **4.3.4. Methods to improve heat transfer**

It is necessary to eliminate, or at least, suppress HTD to avoid the cladding material from overheating. Some methods have been tested which focused on destroying the high-temperature blocking layer attached to the wall by disturbing or swirling the flow using grid spacers, wire-wrapped spacers or spiral ribs on the wall surface [111, 112]. Li et al. [61] experimentally investigated the heat transfer from a wire-wrapped rod to SCW. They found that the annular channels with and without wrapped wires nearly produce the same Nusselt numbers, demonstrating a negligible enhancement induced by the wire-wrapped spacer at normal heat transfer conditions. However, the onset of HTD was postponed to downstream regions due to the existence of the wires. Subsequently, Gang et al. [62], Yang et al. [63] and Wang et al. [113] performed a set of heat-transfer experiments in annular channels with gaps of 2 mm, 4 mm and 6 mm using either wire-wrapped spacers or grid spacers. Unlike Li et al. [61], they concluded that the effects of spacer on heat transfer strongly depend on the mass flux. The heat transfer enhancement diminishes with increasing distance from the spacer. The HTD occurring in the bare-rod annulus was not observed in the wire-wrapped channel. Zhao et al. [73] specially studied the heat transfer of SCW in a 3.65 mm-gap annular channel with two types of grid spacer. They reported that the

heat transfer is enhanced at the downstream of the spacer, but the enhancement decays exponentially until a length of 40 times of  $D_{hy}$ . Zhu et al. [114, 115] numerically investigated the local heat transfer behaviors induced by a standard grid spacer and a grid spacer with split-vanes. Unfavorable results were presented that both of the two spacers lead to an impaired heat transfer in certain regions downstream from the spacers. It was concluded that solely using the grid spacer to reduce the cladding temperature is insufficient.

The effects of spacer on heat transfer of SCW in rod bundles have also been studied. Wang et al. [71] compared the circumferential wall-temperature distribution and the average heat-transfer effectiveness between a bare-rod bundle and a wire-wrapped rod bundle. The maximum wall temperature in the circumference is lowered due to the introduction of the wire wrapping. In addition, the average heat transfer coefficient rises in the wire-wrapped rod bundle especially in the pseudo-critical region, suggesting that heat transfer is improved by the spacer. Grid spacers were used in the experiment of Li et al. [64] with SCW flowing inside a 2×2 rod bundle. A significant drop in the wall temperature was detected after the grid spacer. Gu et al. [70] observed HTD in a 2×2 wire-wrapped rod bundle at a low mass flux of 510 kg/m<sup>2</sup>s. Compared with the bare-rod bundle, they found that the enhanced effect induced by the spacer is more pronounced at high mass fluxes and becomes less effective with decreasing mass flux.

Grid spacer and wire-wrapped spacer can enhance heat transfer to some extent, but the enhancement depends on the flow conditions. A proper spacer is able to suppress the occurrence of HTD. It is noted that the methods for improving heat transfer are not restricted to spacers. Kurganov et al. [116] stated that a relatively higher wall roughness significantly postpones the onset of HTD, and the critical heat flux could be increased by 15%-20%. Nevertheless, the magnitude of HTD becomes more severe once the heat flux exceeds the critical value. Thus, sufficient knowledge is required before putting this kind of improvement method into practice.

## 5. Numerical simulation

### 5.1. Overview of recent numerical studies

To study the mechanisms of the unusual heat transfer near the pseudo-critical temperature, just the macroscopic experimental data (i.e. wall temperature, bulk temperature and heat transfer coefficient) are inadequate. In this case, CFD serves as a necessary supplement to the experiment because it can provide the detailed flow and turbulent information. Abundant efforts have been made in the last decade within the frame of developing SCWRs. The applicability of several CFD codes and a number of turbulence models have been assessed in various flow geometries. The numerical results usually capture the trend of the experimental data qualitatively, but may show considerable discrepancy in certain conditions. Table 4 summarizes the recent numerical works on heat transfer of SCW in normal and enhanced heat-transfer regimes.

(Insert Table 4)

As pointed out by Cheng et al. [117], the main challenge in numerical analysis is the modeling of turbulence at supercritical pressures wherein the thermophysical properties show strong and non-linear variations. Available turbulence models were developed mainly for constant-property flow at normal pressures, but none is reported specially for supercritical fluids. Seo et al. [57] numerically studied the heat transfer of SCW in a vertical tube using the standard  $k-\varepsilon$  model [143]. The results showed good agreements with the experimental data of Yamagata et al. [19]. They concluded that the standard  $k-\varepsilon$  model could serve as a basic model in predicting heat transfer of SCW. This viewpoint is supported by Zhang et al. [124] who compared the standard  $k-\varepsilon$ , Re-Normalization Group (RNG)  $k-\varepsilon$  [144] and realizable  $k-\varepsilon$  models against the experimental data of Yamagata et al. [19] for a horizontal flow. The standard  $k-\varepsilon$  model provides more accurate predictions than the other two models. The usage of RNG  $k-\varepsilon$  model by Lei et al. [127] and Gao and Bai [138] were based on the recommendation of Kim et al. [145] who studied more than 10 first-order turbulence models in FLUENT. Good agreements were found compared with the data of Yamagata et al. [19]. In addition, Wang et al. [113] reported that the predicted heat

transfer coefficients by RNG  $k$ - $\varepsilon$  model are satisfying against the experimental data obtained from an annular channel. Cheng et al. [117] examined four  $\varepsilon$ -type and two  $\omega$ -type turbulence models in CFX and found that the  $\varepsilon$ -type model with scalable wall function are less sensitive to the mesh structure, while the  $\omega$ -type model with automatic wall function failed to reproduce the experimental data. The anisotropic Speziale-Sarkar-Gatski (SSG) Reynolds stress model was recommended for the application of sub-channel geometry due to its capability in capturing second flows. The subsequent studies of Gu et al. [120] and Wang et al. [135] further add confidence to this recommendation.

It is seen in Table 4 that researchers have different recommendations regarding the turbulence model. This may be attributed to the following reasons. Firstly, the selection of a proper turbulence model depends on the flow geometry. For the simple geometry like a circular tube, usually the standard  $k$ - $\varepsilon$  model can return good results. However, in complex geometries such as a sub-channel or a rod bundle, large-scale flow pulsation and local secondary flow may exist [146]. These flow structures could only be predicted by anisotropic turbulence models [117]. More and more studies [129, 147-150] support this viewpoint that anisotropic turbulence models provide more realistic predictions and should be adopted in the CFD analysis of SCWRs. It is worth noticing that while the prediction of turbulent statistics can be improved, the heat transfer coefficients do not differ notably from those obtained by isotropic turbulence models [148, 150]. The second reason is the near-wall treatments coupled with turbulence models. There are two alternative treatments of the near-wall turbulent layer, one is the wall function and the other is the full resolution scheme [151]. For the former, the viscous sublayer and buffer layer (see Fig. 7) are not resolved numerically. Instead, the numerical variable in the near-wall region and the quantities at the wall are connected by semiempirical wall functions. This method allows for a much course grid resolution ( $y^+ \geq 30$ ) and is usually adopted in high- $Re$  models. For the latter, the turbulent boundary layer is fully-resolved with large numerical effort ( $y^+ \leq 1$ ), and low- $Re$  turbulence models are required. In many cases, full resolution is required to better capture the drastic property variations within the

boundary layer, which confines the choice of the turbulence model. The third reason is that the tested flow and thermal conditions vary case to case. The selected heat flux, mass flow rate, tube diameter and flow direction significantly affect the predictions. Existing investigations [118, 128, 150, 153] indicated that both the high- $Re$  models with wall function and the low- $Re$  models with full resolution produce comparable results for normal and enhanced heat-transfer regimes. Nevertheless, the deviation from the experimental data becomes notable with increasing  $q/G$  due to the strong effects of buoyancy. The limited tested ranges result into various recommendations of the turbulence model. Finally, many studies listed in Table 4 drew their conclusions based on the validation with old experimental data such as those from Yamagata et al. [19]. Agreement with the data does not necessarily mean that the average velocity, temperature distribution and turbulent statistics in the radial and axial directions are sufficiently resolved [154]. Thus, newly-obtained experimental data with sufficient accuracy should be incorporated as benchmarks in evaluating various turbulence models applicable for SCW.

(Insert Figure 7)

## 5.2. Modeling of heat transfer deterioration

Challenges are encountered in predicting HTD which is associated with strong buoyancy, thermal acceleration as well as the sharp variations in the thermophysical properties. Turbulence models that are applicable in normal and enhanced heat-transfer regimes may show large discrepancy in predicting HTD. Therefore, it is important to examine the available turbulence models against the heat-transfer data collected in deteriorated regime. Table 5 tabulates the recent studies with this aim, based on which several interesting findings should be discussed.

(Insert Table 5)

High- $Re$  turbulence models, such as the standard  $k-\varepsilon$  model which provides acceptable predictions for normal and enhanced heat transfer, are no longer recommended in modeling the HTD at supercritical pressures. The main reason lies in the standard wall function utilized in these models. There are three major drawbacks

in the standard wall function [57]: i) all the thermophysical properties are assumed to be constant; ii) the buoyancy term and density fluctuation are neglected, and iii) the empirical coefficients were developed for fluids with constant properties. In fact, the numerical simulations of Palko and Anglart [104, 107], Zhang et al. [106], Kiss and Aszódi [150] and Sharabi and Ambrosini [153] indicated that turbulence models relying on wall function cannot predict HTD. This makes sense because HTD is a typical boundary-layer phenomenon while any property variation and buoyancy effect will be neglected if the standard wall function is introduced. However, Seo et al. [57] argued that, since the standard  $k$ - $\varepsilon$  model is reliable in predicting the heat transfer in normal and enhanced regimes, efforts should be made to modify the wall function and include variable properties and transpiration-like effects rather than concentrating on testing the turbulence models. Laurien [151] also believed that the standard wall function could be extended to supercritical fluids with variable properties. He improved the wall function by integrating the energy equation over the viscous sub-layer with its laminar flow, and by modifying Prandtl's mixing length theory [163] for the logarithmic layer with a probability density function for the specific heat [164]. The new function improves the prediction of the wall temperature, but still underpredicts the peak obtained by Ornatskij et al. [130]. More efforts are needed to develop an applicable wall function for supercritical fluids.

The shear stress transport (SST)  $k$ - $\omega$  model [165] has been widely used in the prediction of HTD [77, 89, 104, 107, 108]. This eddy-viscosity model utilizes the standard  $k$ - $\omega$  model in the near wall region (sub- and log- layers) and gradually switches to the standard  $k$ - $\varepsilon$  model in the fully turbulent region [134]. Switching between the two models is performed using the so-called blending function [166]. Thus, the SST  $k$ - $\omega$  model incorporates both the accuracy in the near-wall region and the robustness in the core flow. Palko and Anglart [104, 107] numerically studied the HTD in vertical tubes using this model and compared the predicted wall temperatures with data from Shitsman [22] and Ornatskij et al. [130]. The two peaks in the wall temperature [22] were captured with reasonable accuracy. In addition, the onset of HTD and the maximum wall temperature in Ornatskij et al. [130] were also predicted

successfully, except for the subsequent recovery process. They concluded that the SST  $k-\omega$  model is fully capable in modeling HTD and is recommended for further investigation. Subsequently, similar results were reproduced by several investigations [89, 108, 150, 158, 161]. Selected results are illustrated in Fig. 8 which was taken directly from Liu et al. [89] and Fig. 9 which was reproduced from Palko and Anglart [107]. It is further concluded from these comparisons that the effects of buoyancy play a dominant role in the occurrence of HTD at low mass fluxes, but is negligible at high mass fluxes.

(Insert Figure 8)

(Insert Figure 9)

Apart from the SST  $k-\omega$  model, some low- $Re$  turbulence models are frequently utilized in predicting HTD at supercritical pressures. Sharabi and Ambrosini [153] tested 10 turbulence models using an in-house code THEMAT. They found that the selected six low- $Re$  models provide similar predictions, but tend to overestimate the buoyancy resulting much higher wall temperatures compared to the experimental data. Wen and Gu [156] conducted a numerical analysis using five low- $Re$  models and the SST  $k-\omega$  model. The results were compared with the experimental data of Shitsman [22] and Pis'menny et al. [30]. They demonstrated that all of the five low- $Re$  models qualitatively predict the trend of HTD in the upward and downward flows, but show large discrepancies quantitatively. Mohseni and Bazargan [109] examined six low- $Re$  turbulence models against the data of Yamagata et al. [19] collecting from enhanced heat-transfer regime and the data of Song et al. [79] collecting from deteriorated heat-transfer regime. They reported that the low- $Re$  models of MK, CK and CH predict the enhancement with reasonable accuracy, whereas only the MK model returns an acceptable prediction in the case of HTD. The deviations are mainly originated from the various damping functions utilized as well as the empirical coefficients in the turbulence models. Zhang et al. [106] assessed five low- $Re$  turbulence models and the SST  $k-\omega$  model against the benchmark data

gathered from vertically upward and downward flows. Over-predictions of the experimental wall temperature were observed and only the trends were matched.

As discussed above, most of the numerical analyses on HTD evaluated the applicability of turbulence models using the benchmark data of Shitsman [22], Ornatskij et al. [130] and Pis'menny et al. [30]. The SST  $k-\omega$  model and low- $Re$  model are the two models which may be used as basics for modification. However, these two turbulence models still need further improvements. For the SST  $k-\omega$  model, all existing assessments are restricted to vertical tubes with a simplified 2D geometry. The onset point of HTD and the maximum wall temperature could be captured approximately, but the subsequent decay to normal heat transfer has not been successfully predicted. Moreover, according to Lei et al. [159], SST  $k-\omega$  model is not the best choice to predict HTD in horizontal tubes due to the strong second flows induced by buoyancy. For the low- $Re$  turbulence models, current investigations signified that the trend of HTD could be captured qualitatively but not quantitatively. The deviation from the experimental data varies from model to model and depends on the empirical coefficients. Finally, the prediction accuracy provided by the two models is largely affected by the choice of the turbulent Prandtl number ( $Pr_t$ ). An optimal value of  $Pr_t$  for SCW is still case-dependent.

### 5.3. Improvements to the modeling of turbulent heat flux

#### 5.3.1. Variable turbulent Prandtl number

From Reynolds analogy [167] we know that the heat transfer is related to fluid flow by molecular Prandtl number ( $Pr$ ), assuming that the transfer of energy and momentum are similar in appearance. In a turbulent flow, the turbulent Prandtl number which is defined as the ratio of turbulent viscosity and turbulent diffusivity, is introduced to account for the turbulence contribution to energy transfer. The turbulent Prandtl number shows its influence on heat transfer in two aspects. On the one hand, turbulent heat flux is produced in the energy equation due to the fluctuations of the velocity and temperature, which is usually expressed as  $q_t = -\frac{\mu_t}{Pr_t} \frac{\partial \bar{e}}{\partial x_i}$ . On the other hand, the production of turbulent kinetic energy due to buoyancy,  $G_k = -g\overline{\rho'u'_i} =$

$\beta g \frac{\mu_t}{Pr_t} \frac{\partial \bar{f}}{\partial x_i}$ , is also related to  $Pr_t$ . Note that Boussinesq assumption [168] was used for the two expressions. In most of the numerical simulations mentioned above, the  $Pr_t$  was set to a value close to 0.85. This is ideal for the fluid with constant properties, but is inadequate for SCW because its thermophysical properties undergo drastic variations near the pseudo-critical temperature. An increasing number of researches [10, 132, 169-171] believe that a constant  $Pr_t$  leads to a large error in predicting HTD at supercritical pressures. Fig. 10 shows the comparison between the measured wall temperatures from Gu et al. [43] and the predictions using the SST  $k-\omega$  model with different  $Pr_t$  [172]. It is seen that the predicted wall temperatures are sensitive to the change of  $Pr_t$ , and a constant value of 0.85 fails to accurately capture the experimental data.

(Insert Figure 10)

Hasan [173] found that the thickness of the thermal sublayer decreases with Reynolds number and molecular Prandtl number. Based on a theoretical study, he believed that the  $Pr_t$  should be less than 0.7. Bazargan and Fraser [169] argued that directly determining the  $Pr_t$  for SCW is impracticable because it is impossible to measure the turbulent shear stress, velocity profile, turbulent heat flux and temperature profile at the same time. Their assessment indicated that a larger  $Pr_t$  results into a higher wall temperature and consequently a lower heat transfer coefficient. Mohseni and Bazargan [170] examined four correlations of  $Pr_t$  using the experimental data obtained from SCW and CO<sub>2</sub>, covering normal, enhanced and deteriorated heat-transfer regimes. They found that the effects of  $Pr_t$  on heat transfer are significant outside the laminar sublayer. Most correlations provide reliable heat transfer coefficients only in normal and enhanced regimes. In a subsequent work, Mohseni and Bazargan [174] proposed a new model to calculate the  $Pr_t$  which is applicable for various supercritical fluids. The effects of heat flux, mass flux, pressure, tube diameter, working fluid and bulk temperature were considered in this model. They reported that the predicted heat transfer coefficient is considerably improved using this correlation regardless of whichever low- $Re$  turbulence model is

used. Bae [171] stated that the  $Pr_t$  is far below 1.0 in the boundary layer for supercritical fluids and should be a function of the flow and thermal parameters as well as the physical properties. Based on the mixing-length theory [163], a new formulation was developed by taking the property variation into account. The computational results agreed well against the data collected from SCW, CO<sub>2</sub> and R22. The recovery from deteriorated to normal heat transfer was also successfully reproduced. Tian et al. [172] theoretically and numerically studied the effects of  $Pr_t$  on heat transfer of supercritical fluids. They believed that the region where  $y^+ = 5-100$  plays the most important role on heat transfer. A variable  $Pr_t$  model relating to the local flow conditions and the physical properties was developed. The validations against the experimental data collected from SCW, CO<sub>2</sub> and R134a showed an improved prediction in the wall temperature. Table 6 summarizes the aforementioned assessed and proposed models in calculating the  $Pr_t$ . The development of variable  $Pr_t$  for supercritical fluids is relatively new, and current evaluations are mostly focused on surrogate fluids. More assessments to these models are demanded using the experimental data of SCW.

(Insert Table 6)

### 5.3.2. Algebraic Heat Flux Model

Modeling the turbulent heat flux by  $Pr_t$  is not the only way. There are three methods to calculate the turbulent heat flux. The first method is the Simple Gradient Diffusing Hypothesis model (SGDH), in which the turbulent heat flux is related to the mean temperature gradient and the flow direction. Associating the turbulent heat flux with  $Pr_t$  in Section 5.3.1 belongs to this approach. The second method is the so-called Generalized Gradient Diffusion Hypothesis model (GGDH) which was originally developed from a second-order closure model. In this model, the turbulent heat flux, expressed as  $q_t = -C_t \frac{k}{\varepsilon} \overline{u'_i u'_j} \frac{\partial \bar{E}}{\partial x_j}$ , is determined by the axial and radial temperature gradients. The third method is the Algebraic Heat Flux Model (AHFM) which is calculated as follows [179]:

$$\overline{u'_i t'} = -C_t \frac{k}{\varepsilon} \left[ C_{t1} \overline{u'_i u'_j} \frac{\partial \bar{t}}{\partial x_j} + (1 - C_{t2}) \overline{u'_j t'} \frac{\partial \bar{u}_i}{\partial x_j} + (1 - C_{t3}) \beta g_i \overline{t'^2} \right] \quad (2)$$

It is seen that the AHFM requires the calculation of temperature variance,  $\overline{t'^2}$ , which cannot be obtained by simple two-equation turbulence models. Additional equations [106, 180, 181] have to be introduced to solve the temperature variance and its dissipation rate.

Several investigations [106, 182, 183] showed that the turbulent heat flux is seriously underestimated by SGD model because the temperature change along the flow direction is negligible compared to that in the radial direction. Xiong and Cheng [184] found that the variable  $Pr_t$ , though an attractive solution, improves the modeling of turbulent heat flux limitedly since it is mainly related to SGD which cannot predict the anisotropic turbulent structures. The GGD model is more accurate than SGD model, but still under-predicts the buoyancy term. Therefore, more and more studies [106, 182-184] pay attention to the four-equation turbulence models and utilize the advanced AHFM to improve the numerical predictions.

Zhang et al. [106] performed a heat transfer experiment using SCW and vertically upward and downward flows. Conventional low- $Re$  turbulence models and the SST  $k-\omega$  model failed to reproduce the wall temperature trend, but the experimental data were captured satisfactorily once the AHFM was adopted to model the buoyancy term. Xu et al. [182] examined different combinations of SGD, GGD and AHFM in the turbulent kinetic energy equation. They found that all of the three models return good predictions in the enhanced heat transfer regime, but none of these models is accurate in the case of DHT. They concluded that the selection of a suitable turbulence model is more important than modeling the buoyancy term. In the above-mentioned two studies, the AHFM was introduced only in the momentum equation to model the buoyancy term, whereas the turbulent heat flux in the energy equation was still closed with  $Pr_t$  and SGD model. Xiong and Cheng [184] confirmed that the numerical prediction could be further improved by introducing the AHFM into the energy equation. They employed various combinations of SGD, GGD, AHFM and Elliptic Blending AHFM (EB-AHFM) in predicting the buoyancy

and turbulent heat flux, and compared the predictions with the direct numerical simulation (DNS) of Bae et al. [185]. It was found that the EB-AHFM is superior to other models and could be regarded as a candidate for further optimization.

Recently, using an in-house code THEMAT and CFD code STAR-CCM+, Pucciarelli et al. [186, 187] evaluated the performance of AHFM in modeling buoyancy based on the comparisons with a wide range of the experimental data as well as the DNS results. Due to the restriction of the commercial code, the AHFM was not fully implemented into the energy equation in STAR-CCM+, but was used to develop an improved model for the  $Pr_t$ . The assessments showed that the prediction accuracy depends on the selected turbulence model and the set of coefficients in AHFM. It is impossible to identify a single set of parameters applicable to all the flow conditions. Papp et al. [183] found that the coefficient  $C_{t3}$  in AHFM determines the magnitude of HTD (wall temperature peak) while  $C_t$  has a great effect on its onset point. Based on the evaluation, they believed that AHFM has the real capability in simulating the distribution of turbulent heat flux. Similar to the findings of Pucciarelli et al. [186, 187], however, a single set of parameters is insufficient in dealing with the wide range of flow conditions. In a more recent work, Pucciarelli and Ambrosini [179] proposed a dynamic definition of the coefficients in the AHFM using a dimensionless enthalpy  $H^*$  which is defined as  $H^* = \frac{\beta_{pc}}{c_{p,pc}}(H - H_{pc})$ . Thus, the constant coefficient of  $(1 - C_{t3})$  in Eq. (2) was replaced by the dynamic definition of  $C_{t4} = 1 - C_{t3} = \text{Max}\left(0, e^{\frac{H^*}{2.5}} - 0.4\right)$ . Significant improvements in the prediction of HTD have been observed for many sources of experimental data, some of which were reproduced in Fig. 11.

(Insert Figure 11)

#### 5.4. Advanced simulations of LES and DNS

All aforementioned numerical studies are based on Reynolds-Averaged Navier-Stokes (RANS) equations which are time-averaged equations for the fluid flow. To close the equation set, a proper turbulence model is needed. However,

applying the constant-property-based turbulence model to supercritical fluids is not straightforward due to the severe variations in the thermophysical properties. DNS is an advanced simulation method which solves the Navier-Stokes equations directly without any assumptions. Since the whole range of the turbulence in the spatial and temporal scales are fully resolved, detailed information about the flow becomes available compared to the time-averaged values in RANS. The only limitation of DNS is the huge amount of computing resources and time, even for the flow with low Reynolds numbers. Currently, this method has been applied to study the heat transfer phenomenon of supercritical CO<sub>2</sub> [185], but none is reported for SCW. An alternative method is the large eddy simulation (LES) [190], which reduces the computational cost by resolving only the large-scale eddies. A filtering function is used to distinguish between the large and small scales. Although LES is computationally cheaper than DNS, applying this method to investigate the heat transfer of SCW is still rarely seen in publication. Ničeno and Sharabi [191] performed LES to study the flow behavior and heat transfer of SCW in upward and downward tubes. Since the heat transfer to supercritical fluids is inherently unstable due to the variation in the properties, a sufficiently fine mesh is needed especially in the near wall region. The numerical results were compared with the experimental data produced by Pis'menny et al. [30], which showed that LES is able to predict the HTD in terms of the onset point, the magnitude as well as the recovery to normal heat transfer. The detailed information about the mean flow and turbulent statistics also helps to evaluate turbulence models in RANS.

At present, CFD studies on the heat transfer to SCW are still focused on RANS which allows incorporating complex geometries with a large fluid domain. DNS and LES are more appropriate to analyze the physical mechanisms of the unusual heat transfer phenomena. It is noted that the experimental measurements other than wall temperature, such as the distributions of velocity and Reynolds stresses, are scarce and highly needed to validate existing numerical simulations.

## 6. Prediction methods

An accurate prediction of the heat transfer from a fuel assembly to SCW affects the thermal-hydraulic design of SCWRs. Since the 1950s, a number of heat-transfer correlations have been proposed, most of which were reviewed by Piro et al. [11] and assessed by Jager et al. [192]. The majority of these correlations were developed for circular tubes in support of the design of supercritical boilers, but very few for rod bundles owing to the lack of relevant experimental data. In addition, most correlations can well estimate the heat transfer coefficient in normal and enhanced heat transfer regimes, but none is able to accurately predict the onset and magnitude of HTD [11, 42]. The correlations of Bishop et al. [23], Swenson et al. [24] and Jackson [44] are most frequently recommended. The former two correlations can be used in the preliminary design of SCWRs because the applicable ranges match the SCWR operating parameters [35].

Current heat-transfer correlations could be roughly divided into three types. The first type was developed based on the expression of Dittus-Boelter [16] correlation. To account for the drastic variation in the thermophysical properties of SCW, additional terms such as  $\left(\frac{\rho_w}{\rho_b}\right)^m$  or  $\left(\frac{\mu_w}{\mu_b}\right)^n$  are added into the correlation with the exponent  $m$  and  $n$  being fitted by the experimental measurements. The second type takes the friction factor into the correlation based on the idea that heat and momentum transfer can still be analogized at supercritical pressures. This type of correlation was mainly developed by Russian researchers between the 1970s-1990s, such as the correlations of Krasnoshchekov et al. [72] and Petukhov et al. [31]. The third type was proposed to address the effects of buoyancy and thermal acceleration on heat transfer to supercritical fluids. Non-dimensional parameters such as the buoyancy factor  $Bo$  and acceleration factor  $Ac$  are usually incorporated. Examples are the correlations of Cheng et al. [42] and Liu and Kuang [193].

Table 7 summarizes the heat transfer correlations developed for SCW since 2005. Cheng et al. [42] focused on creating an amendatory term  $F$  to the Dittus-Boelter correlation [16]. Three non-dimensional factors,  $\pi_A$ ,  $\pi_B$  and  $\pi_C$  were derived to account for the effects of thermal acceleration, buoyancy and property

variation, respectively. The acceleration factor  $\pi_A$  was found most important while the other two factors could be expressed indirectly by  $\pi_A$ . The variables depending on the wall temperature were eliminated in this correlation to avoid iteration and numerical instability. Gupta et al. [18] developed a heat-transfer correlation using the experimental data of Kirillov et al. [137]. The wall temperature was utilized as the reference temperature, which is consistent with the method of Swenson et al. [24]. Mokry et al. [35] proposed a correlation for heat transfer of SCW in tubes based on dimension analysis. They suggested using cross-sectional average Prandtl number ( $\overline{Pr}$ ) instead of  $Pr$  to better address the thermophysical property variations across a cross-section. Liu and Kuang [193] collected 14758 experimental data points on heat transfer of SCW in vertically upward tubes, covering a wide range of experimental parameters and tube diameters. A new correlation was proposed considering the effects of buoyancy, thermal acceleration as well as the thermophysical property variations. The correlation of Chen and Fang [194] was developed based on 5366 experimental data points collected from 13 publications for vertical tubes and is applicable for normal, enhanced and deteriorated heat transfer regimes. A recent study [195] demonstrated a superior performance of this correlation in predicting the heat transfer of SCW in a bare rod bundle. Deev et al. [101] summarized available publications related to the heat transfer from annuli and rod bundle to SCW. Based on the analysis of the experimental data, they put forward a correlation specifically for these sub-channel geometries.

(Insert Table 7)

For the purpose of developing heat transfer correlations, attentions need to be paid to the following issues. Firstly, the ratio of  $\frac{\bar{c}_p}{c_{pb}}$  was found most effective in correlating the experimental data [11, 19, 42, 43], and thus could be incorporated into the expressions. Also, introducing excessive amendatory terms does not significantly improve the prediction. For example, the complex correlation of Liu and Kuang [193] shows a limited improvement to a simple correlation like the one developed by Bishop et al. [23] or Jackson [44] in predicting the heat transfer coefficient in a  $2 \times 2$

rod bundle [195]. Secondly, the bulk temperature is recommended as the reference temperature. Mokry and Piroo [196] derived three empirical correlations using the bulk temperature, wall temperature and film temperature (average temperature between the wall and bulk) as the reference temperatures, respectively, and assessed the three correlations with the same set of experimental data. The comparison showed that the predictions given by the bulk-temperature-based correlation agree accurately with the data. Thirdly, the entrance effects or upstream effects on heat transfer of SCW need to be considered. As discussed in Section 4.2.5, several investigations have shown that these effects are more pronounced for supercritical fluids compared to fluids with constant properties. A proper geometry-based term is needed to account for the effects of inlet condition. Finally, multi solutions may exist at supercritical pressures [42]. That is, the wall temperature has different values under the same experimental conditions, i.e. channel geometry, pressure, mass flux, heat flux and bulk temperature. This phenomenon is considered to be one of the reasons for the large discrepancy of the experimental data coming from different sources [17]. Parameters depending on the wall temperature are not recommended in developing new correlations because this might involve iterations and numerical instability.

## 7. Conclusions

The state-of-the-art R&D on heat transfer to SCW in simple geometry and bundle subassemblies has been presented through an extensive review of recent publications. Based on the analyses, the following conclusions could be drawn.

A large number of experimental studies [27, 29, 33, 34, 55, 61-63] have been performed with simple geometry such as tubes and annuli. Effects of flow conditions, diameter (or flow area), flow direction and spacers on heat transfer were investigated extensively and confirmed with observations in previous studies. Experimental data obtained from these studies are ideal for validating correlations and analytical tools, or for developing new prediction methods.

Several experimental studies on heat transfer to SCW have been performed with bundle subassemblies [58-60, 66-68, 70, 71]. The observed heat transfer

characteristics are similar to those in simple tubes. However, the heat transfer in bundles appears to be improved compared to that in tubes at similar cross-sectional-averaged flow conditions. One of the major concerns has been the mal-distribution of wall temperature around the heated rod of the bundle, which could lead to rod distortion affecting the thermal-hydraulic performance. Experimental results indicated a relatively small circumferential temperature gradient within the range of test conditions.

Heat transfer correlations adopted the form of Dittus-Boelter correlation [16] with additional terms to account for variations in thermophysical properties. Most of these correlations provide reasonable predictions of heat transfer coefficients in normal and enhanced heat-transfer regimes, but not for the HTD. Several issues were encountered in developing correlations (e.g., the need of information based on wall temperature and heat flux that require iteration and could lead to multiple solutions).

Experimental and numerical studies demonstrated that the HTD depends strongly on buoyancy [77, 89, 161], thermal acceleration [12, 64] and variation in the thermophysical properties [20, 56, 76]. Correlations proposed by Lokshin et al. [94] and Mokry et al. [35] are applicable in predicting the transition boundary to HTD in tubes, but tend to underpredict the critical heat flux for annuli and rod bundles. Grid and wire-wrapped spacers enhance the heat transfer and suppress the onset of HTD.

The majority of numerical analyses focus on evaluating the applicability of various turbulence models in predicting the heat transfer to SCW, but none of these models is applicable to a wide range of flow conditions. The high- $Re$  turbulence models adopting wall functions cannot capture the HTD. The SST  $k-\omega$  model and low- $Re$  models coupled with the full resolution scheme are capable to qualitatively capture the onset and magnitude of HTD. However, further improvements are needed, in particular to model the turbulent heat flux which is directly linked to buoyancy and thermal diffusion, through the variable turbulent Prandtl number or other advanced methods (such as AHFM). LES and DNS [185, 191] can be used to study the fundamental heat transfer and flow behaviors at supercritical pressures. However,

significant expansion and investment in computational resources are required to extend their applications.

Other observed issues in improving the prediction accuracy of heat transfer to water at supercritical pressures include the following:

(i) Reliability of heat transfer data in rod bundles. Large scatter has been observed among wall-temperature measurements along the heated rods in bundles [64, 70, 71], and could be attributed to the fluctuation of flow conditions or measurement uncertainty. Besides, while the circumferential variations of the wall temperature were obtained, only the cross-sectional average bulk-fluid temperature was available in calculating the local heat-transfer coefficient. This hampers the effectiveness of using these data for validation of analytical tools (such as subchannel codes or CFD tools).

(ii) Lack of experimental data for quantification the effects of non-uniform axial and circumferential power distributions on heat transfer. All experiments performed up-to-date employed channels with uniform axial and circumferential power distributions, which are not representative to the power profiles of SCWR fuels. The location of the fuel assembly and burnup would lead to axially non-uniform power profiles along the fuel assembly [139]. In addition, the introduction of the water box in the fuel assembly would enhance moderation to the adjacent fuel rods leading to a non-uniform circumferential power profile [164]. The current assumption of negligible upstream history effect on local heat transfer needs to be confirmed or validated.

(iii) Lack of detailed measurements in flow velocity and turbulence at supercritical pressures. These measurements facilitate improvement in understanding the changes in velocity and turbulent distributions within simple and complex geometries, especially local phenomena such as spacer and rod distortion. In addition, correlations for specific separate effects can be developed through applying these local measurements. The measurements are also applicable for benchmarking CFD tools. Performing experiments for detailed measurements in water flow at supercritical pressures are challenging. The use of surrogate fluids would simplify the complexity and lower the cost of these experiments.

(iv) Difficulty in modeling buoyancy. Both the variable  $Pr_t$  model and AHFM appear to be able to capture the local transport effect. Improvements to these models are needed to take into the account of buoyancy using available experimental data. This would enhance the prediction accuracy of heat transfer especially at the DHT regime.

(v) Unsteady nature of the fluid flow and heat transfer at supercritical pressures. Variations of the thermophysical property, especially at the vicinity of the pseudo-critical point, have led to the unsteady flow impacting the heat transfer behaviors. Application of LES, DNS or transient RANS is needed to investigate the phenomena, in particular the HTD.

(vi) Extensive use of non-dimensional parameters and both wall temperature and heat flux as dependent parameters. Some heat transfer correlations include an extensive list of non-dimensional parameters as correlating functions. These functions introduce duplicated effects and hence may not be necessary or relevant. Furthermore, wall-temperature and heat-flux based parameters were included as correlating functions in a few empirical equations. This has introduced additional complexity in applications as iterations are required and in some cases lead to multiple solutions.

### **Acknowledgments**

This research was financially supported by the National Natural Science Foundation of China (11605057), the Fundamental Research Funds for the Central Universities (2018MS046, 2016ZZD05) and China Scholarship Council (CSC). The authors would like to give sincere gratitude to Prof. Yassin A. Hassan of Texas A&M University, for his instructive advice and useful suggestions on this paper.

### **References**

- [1] Y. Liu, Q. Li, X. Duan, et al., Thermodynamic analysis of a modified system for a 1000 MW single reheat ultra-supercritical thermal power plant. *Energy* 145 (2018) 25-37.

- [2] S. Wang, D. Yang, Y. Zhao, et al., Heat transfer characteristics of spiral water wall tube in a 1000 MW ultra-supercritical boiler with wide operating load mode. *Applied Thermal Engineering* 130 (2018) 501-514.
- [3] U.S. DOE, Nuclear Energy Research Advisory Committee and Generation IV International Forum. A Technology Roadmap for Generation IV Nuclear Energy System, 2002.
- [4] Y. Oka, S. Koshizuka, Supercritical-pressure, once-through cycle light water cooled reactor concept. *Journal of Nuclear Science and Technology* 38 (2001) 1081-1089.
- [5] G. Heusener, U. Müller, T. Schulenberg, et al., A European development program for a High Performance Light Water Reactor (HPLWR). Proceedings of the 1st International Symposium on Supercritical Water Cooled Reactor Design and Technology (SCR-2000), Tokyo, Japan, 2000.
- [6] L.K.H. Leung, M. Yetisir, W. Diamond, et al., A next generation heavy water nuclear reactor with supercritical water as coolant. International Conference on Future of Heavy Water Reactors, Canadian Nuclear Society, Canada, 2011.
- [7] Y.D. Baranaev, P.L. Kirillov, V.M. Poplavskii, et al., Supercritical-pressure water nuclear reactors. *Atomic Energy* 96 (2004) 345-351.
- [8] OECD Nuclear Energy Agency, Technology Roadmap Update for Generation IV Nuclear Energy Systems, 2014.
- [9] Y. Su, K.S. Chaudri, W. Tian, et al., Optimization study for thermal efficiency of supercritical water reactor nuclear power plant. *Annals of Nuclear Energy* 63 (2014) 541-547.
- [10] X. Cheng, T. Schulenberg, Heat transfer at supercritical pressures - Literature review and application to a HPLWR. Vol 6609, FZKA, 2001.
- [11] I.L. Piro, H.F. Khartabil, R.B. Duffey, Heat transfer to supercritical fluids flowing in channels - empirical correlations (survey), *Nuclear Engineering and Design* 230 (2004) 69-91.

- [12] I.L. Pioro, R.B. Duffey, Experimental heat transfer in supercritical water flowing inside channels (survey), *Nuclear Engineering and Design* 235 (2005) 2407-2430.
- [13] M.M. Rahman, J. Dongxu, M.S. Beni, et al., Supercritical water heat transfer for nuclear reactor applications: A review. *Annals of Nuclear Energy* 97 (2016) 53-65.
- [14] D. Huang, Z. Wu, B. Sunden, et al., A brief review on convection heat transfer of fluids at supercritical pressures in tubes and the recent progress. *Applied Energy* 162 (2016) 494-505.
- [15] E.W. Lemmon, M.O. McLinden, M.L. Huber, NIST Reference Fluid Thermodynamic and Transport Properties - REFPROP, NIST Standard reference database 23 (on diskette: Executable with Source), Ver. 7.0. U.S. Department of Commerce, 2002.
- [16] F.W. Dittus, L.M.K. Boelter, *Publications of Engineering, University of California* 2 (1930) p. 443.
- [17] X. Cheng, X.J. Liu, R&D challenges of heat transfer to supercritical fluids. The 8th International Symposium on Supercritical Water-cooled Reactors (ISSCWR8), Chengdu, China, March 13-15, 2017.
- [18] S. Gupta, A. Farah, K. King, et al., Developing new heat-transfer correlation for supercritical-water flow in vertical bare tubes. *Proceedings of 18th International Conference on Nuclear Engineering (ICONE-18)*, Xi'an, China, May 17-21, 2010.
- [19] K. Yamagata, K. Nishikawa, S. Hasegawa, et al., Forced convective heat transfer to supercritical water flowing in tubes. *International Journal of Heat and Mass Transfer* 15 (1972) 2575-2593.
- [20] S. Koshizuka, N. Takano, Y. Oka, Numerical analysis of deterioration phenomena in heat transfer to supercritical water. *International Journal of Heat and Mass Transfer* 38 (1995) 3077-3084.
- [21] I.L. Pioro, R.B. Duffey, *Heat Transfer and Hydraulic Resistance at Supercritical Pressures in Power-Engineering Applications*. ASME Press, New York, 2007.

- [22] M.E. Shitsman, Impairment of the heat transmission at supercritical pressures. *High Temperature* 1 (1963) 237-244.
- [23] A.A. Bishop, R.O. Sandberg, L.S. Tong, Forced convection heat transfer to water at near critical temperatures and supercritical pressures. Westinghouse Electric Corporation, Pittsburgh, Pa. Atomic Power Div, 1964.
- [24] H.S. Swenson, J.R. Carver, C.R. Karakala, Heat transfer to supercritical water in smooth-bore tubes. *Journal of Heat Transfer, Trans. ASME* 87 (1965) 477-484.
- [25] D.C. Groeneveld, S. Tavoularis, P. Raogudla, et al., Analytical and experimental program of supercritical heat transfer research at the University of Ottawa. *Nuclear Engineering and Technology* 40 (2008) 107-116.
- [26] P.L. Kirillov, V.A. Grabezhnaya, Heat transfer at supercritical pressures and the onset of deterioration. *Proceedings of 14th International Conference on Nuclear Engineering (ICONE-14)*, Miami, Florida, USA, July 17-20, 2006.
- [27] M. Bazargan, D. Fraser, V. Chatoorgan, Effect of buoyancy on heat transfer in supercritical water flow in a horizontal round tube. *Journal of Heat Transfer* 127 (2005) 897-902.
- [28] B.S. Petukhov, A.F. Polyakof, V.A. Kuleshov, et al., Turbulent flow and heat transfer in horizontal tubes with substantial influence of thermo-gravitational forces. *Proc. 5th International Heat Transfer Conference*, Tokyo, Japan, September 3-7, 1974.
- [29] E.N. Pis'menny, V.G. Razumovskiy, E.M. Maevskiy, Experimental study on temperature regimes to supercritical water flowing in vertical tubes at low mass fluxes. *Proceedings of the International Conference Nuclear Energy Systems for Future Generation and Global Sustainability*, Tsukuba, Japan, October 9-13, 2005.
- [30] E.N. Pis'menny, V.G. Razumovskiy, A.E. Maevskiy, et al., Heat transfer to supercritical water in gaseous state or affected by mixed convection in vertical tubes. *Proceedings of 14th International Conference on Nuclear Engineering (ICONE-14)*, Miami, Florida, USA, July 17-20, 2006.

- [31] B.S. Petukhov, V.A. Kurganov, V.B. Ankudinov, Heat transfer and flow resistance in the turbulent pipe flow of a fluid with near-critical state parameters. *High Temperature* 21 (1983) 81-89.
- [32] F. Yin, T.K. Chen, H.X. Li, An investigation on heat transfer to supercritical water in inclined upward smooth tubes. *Heat Transfer Engineering* 27 (2006) 44-52.
- [33] X.J. Zhu, Q.C. Bi, D. Yang, et al., An investigation on heat transfer characteristics of different pressure steam-water in vertical upward tube. *Nuclear Engineering and Design* 239 (2009) 381-388.
- [34] S. Mokry, I. Pioro, P. Kirillov, et al., Supercritical-water heat transfer in a vertical bare tube. *Nuclear Engineering and Design* 240 (2010) 568-576.
- [35] S. Mokry, I. Pioro, A. Farah, et al., Development of supercritical water heat-transfer correlation for vertical bare tubes. *Nuclear Engineering and Design* 241 (2011) 1126-1136.
- [36] S.Q. Yu, H.X. Li, X.L. Lei, et al., Experimental investigation on heat transfer characteristics of supercritical pressure water in a horizontal tube. *Experimental Thermal and Fluid Science* 50 (2013) 213-221.
- [37] S.Q. Yu, H.X. Li, X.L. Lei, et al., Influence of buoyancy on heat transfer to water flowing in horizontal tubes under supercritical pressure. *Applied Thermal Engineering* 59 (2013) 380-388.
- [38] J.D. Jackson, W.B. Hall, Influences of buoyancy on heat transfer to fluids flowing in vertical tubes under turbulent conditions. *Turbulent Forced Convection in Channels and Bundles*. Hemisphere Publishing Corporation, 613-640, 1979.
- [39] B.S. Petukhov, A.F. Polyakov, *Heat Transfer in Turbulent Mixed Convection*. Hemisphere Publishing Corporation, 1986.
- [40] Z. Shen, D. Yang, G. Chen, et al., Experimental investigation on heat transfer characteristics of smooth tube with downward flow. *International Journal of Heat and Mass Transfer* 68 (2014) 669-676.

- [41] M. Zhao, H.Y. Gu, X. Cheng, Experimental study on heat transfer of supercritical water flowing downward in circular tubes. *Annals of Nuclear Energy* 63 (2014) 339-349.
- [42] X. Cheng, Y.H. Yang, S.F. Huang, A simplified method for heat transfer prediction of supercritical fluids in circular tubes. *Annals of Nuclear Energy* 36 (2009) 1120-1128.
- [43] H.Y. Gu, M. Zhao, X. Cheng, Experimental studies on heat transfer to supercritical water in circular tubes at high heat fluxes. *Experimental Thermal and Fluid Science* 65 (2015) 22-32.
- [44] J.D. Jackson, Consideration of the heat transfer properties of supercritical pressure water in connection with the cooling of advanced nuclear reactors. *Proceedings of the 13th Pacific Basin Nuclear Conference, Shenzhen, China, October 21-25, 2002.*
- [45] X.L. Lei, H.X. Li, W.Q. Zhang, et al., Experimental study on the difference of heat transfer characteristics between vertical and horizontal flows of supercritical pressure water. *Applied Thermal Engineering* 113 (2017) 609-620.
- [46] Z. Shen, D. Yang, S.Y. Wang, et al., Experimental and numerical analysis of heat transfer to water at supercritical pressures. *International Journal of Heat and Mass Transfer* 108 (2017) 1676-1688.
- [47] X. Cheng, T. Schulenberg, D. Bittermann, et al., Design analysis of core assemblies for supercritical pressure conditions. *Nuclear Engineering and Design* 223 (2003) 279-294.
- [48] P. Wu, J. Gou, J. Shan, et al., Safety analysis code SCTRAN development for SCWR and its application to CGNPC SCWR. *Annals of Nuclear Energy* 56 (2013) 122-135.
- [49] S. Kumar, P.K. Vijayan, U. Kannan, et al., Experimental and computational simulation of thermal stratification in large pools with immersed condenser. *Applied Thermal Engineering* 113 (2016) 345-361.

- [50] X.J. Liu, T. Yang, X. Cheng, Development and assessment of a sub-channel code applicable for trans-critical transient of SCWR. *Nuclear Engineering and Design* 262 (2013) 499-509.
- [51] R.V. Maitri, C. Zhang, J. Jiang, Computational fluid dynamic assisted control system design methodology using system identification technique for CANDU supercritical water cooled reactor (SCWR). *Applied Thermal Engineering* 118 (2017) 17-22.
- [52] S. Zwolinski1, M. Anderson, M. Corradini, et al., Evaluation of fluid-to-fluid scaling method for water and carbon dioxide at supercritical pressure. The 5th International Symposia on SCWR (ISSCWR-5), Vancouver, British Columbia, Canada, March 13-16, 2011.
- [53] B.V. Dyadyakin, A.S. Popov, Heat transfer and thermal resistance of tight seven-rod bundle, cooled with water flow at supercritical pressures. *Transactions of VTI* 11 (1977) 244-253.
- [54] V.A. Silin, V.A. Voznesensky, A.M. Afrov, The light water integral reactor with natural circulation of the coolant at supercritical pressure B-500 SKDI. *Nuclear Engineering and Design* 144 (1993) 327-336.
- [55] J. Licht, M. Anderson, M. Corradini, Heat transfer to water at supercritical pressures in a circular and square annular flow geometry. *International Journal of Heat and Fluid Flow* 29 (2008) 156-166.
- [56] J.D. Jackson, W.B. Hall, Forced convection heat transfer to fluids at supercritical pressure. *Turbulent Forced Convection in Channels and Bundles*. Hemisphere Publishing Corporation, 563-611, 1979.
- [57] K.W. Seo, M.H. Kim, M.H. Anderson, et al., Heat transfer in a supercritical fluid: classification of heat transfer regimes. *Nuclear Technology* 154 (2006) 335-349.
- [58] V.G. Razumovskiy, E.N. Pis'menny, A.E. Koloskov, et al., Heat transfer to supercritical water in vertical 7-rod bundle. In 16th International Conference on Nuclear Engineering (ICONE-16). Orlando, Florida, USA, May 11-15, 2008.

- [59] V.G. Razumovskiy, E.N. Pis'menny, A.E. Koloskov, A.E., et al., Heat transfer to supercritical water in vertical annular channel and 3-rod bundle. In 17th International Conference on Nuclear Engineering (ICONE-17). Brussels, Belgium, July 12-16, 2009.
- [60] V.G. Razumovskiy, E.M. Mayevskiy, A.E. Koloskov, et al., Heat transfer to water at supercritical parameters in vertical tubes, annular channels, 3-and 7-rod bundles. In 21st International Conference on Nuclear Engineering (ICONE-21). Chengdu, China, July 29 - August 2, 2013.
- [61] H.Z. Li, H.J. Wang, Y.S. Luo, et al., Experimental investigation on heat transfer from a heated rod with helically wrapped wire inside a square vertical channel to water at supercritical pressures. Nuclear Engineering and Design 239 (2009) 2004-2012.
- [62] W. Gang, Q.C. Bi, Z.D. Yang, et al., Experimental investigation of heat transfer for supercritical pressure water flowing in vertical annular channels. Nuclear Engineering and Design 241 (2011) 4045-4054.
- [63] Z.D. Yang, Q.C. Bi, H. Wang, et al., Experiment of heat transfer to supercritical water flowing in vertical annular channels. Journal of Heat Transfer 135 (4) (2013).
- [64] H.B. Li, M. Zhao, H.Y. Gu, et al., Experimental research of supercritical water heat transfer in different channels. In 21st International Conference on Nuclear Engineering (ICONE-21). Chengdu, China, July 29 - August 2, 2013.
- [65] M. Zhao, H.B. Li, J. Yang, et al., Experimental study on heat transfer to supercritical water flowing through circular tubes and 2×2 rod bundles. In Proceedings of the 6th International Symposium on Supercritical Water-Cooled Reactors (ISSCWR-6), Shenzhen, China, March 3-7, 2013.
- [66] H. Wang, Q.C. Bi, L.C. Wang, et al., Experimental investigation of heat transfer from a 2×2 rod bundle to supercritical pressure water. Nuclear Engineering and Design 275 (2014) 205-218.

- [67] H.Y. Gu, Z.X. Hu, D. Liu, et al., Experimental studies on heat transfer to supercritical water in 2×2 rod bundle with two channels. *Nuclear Engineering and Design* 291 (2015) 212-223.
- [68] H.Y. Gu, H.B. Li, Z.X. Hu, et al., Heat transfer to supercritical water in a 2×2 rod bundle. *Annals of Nuclear Energy* 83 (2015) 114-124.
- [69] J.D. Jackson, J. Fewster, Forced convection data for supercritical pressure fluids. *Heat Transfer and Fluid Flow* 21540, 1975.
- [70] H.Y. Gu, Z.X. Hu, D. Liu, et al., Experimental study on heat transfer to supercritical water in 2×2 rod bundle with wire wraps. *Experimental Thermal and Fluid Science* 70 (2016) 17-28.
- [71] H. Wang, Q.C. Bi, L.K.H. Leung, Heat transfer from a 2×2 wire-wrapped rod bundle to supercritical pressure water. *International Journal of Heat and Mass Transfer* 97 (2016) 486-501.
- [72] E.A. Krasnoshchekov, V.S. Protopopov, F. Van, et al., Experimental investigation of heat transfer for carbon dioxide in the supercritical region. *Proceedings of the 2nd All-Soviet Union Conference on Heat and Mass Transfer, Minsk, Belarus, 1964.*
- [73] M. Zhao, H.Y. Gu, H.B. Li, et al., Heat transfer of water flowing upward in vertical annuli with spacers at high pressure conditions. *Annals of Nuclear Energy* 87 (2016) 209-216.
- [74] J. Licht, M. Anderson, M. Corradini, Heat transfer and fluid flow characteristics in supercritical pressure water. *Journal of Heat Transfer* 131(7) (2009).
- [75] Z. Shen, D. Yang, H. Xie, et al., Flow and heat transfer characteristics of high-pressure water flowing in a vertical upward smooth tube at low mass flux conditions. *Applied Thermal Engineering* (102) 2016 391-401.
- [76] J.G. Wang, H.X. Li, S.Q. Yu, et al., Investigation on the characteristics and mechanisms of unusual heat transfer of supercritical pressure water in vertically-upward tubes. *International Journal of Heat and Mass Transfer* 54 (2011) 1950-1958.

- [77] H. Wang, Q.C. Bi, Z.D. Yang, et al., Experimental and numerical investigation of heat transfer from a narrow annulus to supercritical pressure water. *Annals of Nuclear Energy* 80 (2015) 416-428.
- [78] T. Yamashita, S. Yoshida, H. Mori, et al., Heat transfer study under supercritical pressure conditions. In *Proceedings of the International Conference on Global Environment and Advanced Nuclear Power Plants*, Kyoto, Japan, September 15-19, 2003.
- [79] J.H. Song, H.Y. Kim, H. Kim, et al., Heat transfer characteristics of a supercritical fluid flow in a vertical pipe. *The Journal of Supercritical Fluids* 44 (2008) 164-171.
- [80] Z. Shang, S. Chen, Numerical investigation of diameter effect on heat transfer of supercritical water flows in horizontal round tubes. *Applied Thermal Engineering* 31 (2011) 573-581.
- [81] M.F. Loewenberg, E. Laurien, A. Class, et al., Supercritical water heat transfer in vertical tubes: A look-up table. *Progress in Nuclear Energy* 50 (2008) 532-538.
- [82] J.W. Ackerman, Pseudoboiling heat transfer to supercritical pressure water in smooth and ribbed tubes. *Journal of Heat transfer* 92 (1970) 490-497.
- [83] B. Shiralkar, P. Griffith, The effect of swirl, inlet conditions, flow direction, and tube diameter on the heat transfer to fluids at supercritical pressure. *Journal of heat transfer* 92 (1970) 465-471.
- [84] Y.Y. Bae, H.Y. Kim, D.J. Kang, Forced and mixed convection heat transfer to supercritical CO<sub>2</sub> vertically flowing in a uniformly-heated circular tube. *Experimental Thermal and Fluid Science* 34 (2010) 1295-1308.
- [85] S. Yildiz, D.C. Groeneveld, Diameter effect on supercritical heat transfer. *International Communications in Heat and Mass Transfer* 54 (2014) 27-32.
- [86] J.D. Jackson, Fluid flow and convective heat transfer to fluids at supercritical pressure. *Nuclear Engineering and Design* 264 (2013) 24-40.
- [87] J.D. Jackson, Studies of buoyancy-influenced turbulent flow and heat transfer in vertical passages. In *13th International Heat Transfer Conference*. Begel House Inc., 2006

- [88] Z. Shang, CFD investigation of vertical rod bundles of supercritical water-cooled nuclear reactor. *Nuclear Engineering and Design* 239 (2009) 2562-2572.
- [89] L. Liu, Z. Xiao, X. Yan, et al., Heat transfer deterioration to supercritical water in circular tube and annular channel. *Nuclear Engineering and Design* 255 (2013) 97-104.
- [90] W.B. Hall, J.D. Jackson, A. Watson, Paper 3: A Review of Forced Convection Heat Transfer to Fluids at Supercritical Pressures. *Proceedings of the Institution of Mechanical Engineers*, London, England, SAGE Publications, 1967.
- [91] G. Domin, Heat transfer to water in pipes in the critical/supercritical region. *BWK* 15 (1963) 527-532.
- [92] M.A. Styrikovich, T.K. Margulova, Z.L. Miropol'Skii, Problems in the development of designs of supercritical boilers. *Teploenergetika* 14 (1967) 5-9.
- [93] Y.V. Vikhrev, Y.D. Barulin, A.S. Kon'Kov, A study of heat transfer in vertical tubes at supercritical pressures. *Thermal Engineering* 14 (1967) 116-119.
- [94] V.A. Lokshin, I.E. Semenovk. Y.V. Vikhrev, Calculating temperature conditions of radiant heating surfaces in supercritical boilers. *Thermal Engineering* 15 (1968) 34-39.
- [95] N.S. Kondrat'ev, Heat transfer and hydraulic resistance with supercritical water flowing in tubes. *Thermal Engineering* 16 (1969) 73-77.
- [96] H. Ogata, S. Sato, Measurements of forced convection heat transfer to supercritical helium. *Proceedings of the 4th International Cryogenic Engineering Conference*, Eindhoven, May 24-26, 1972.
- [97] V. Protopopov, I. Kuraeva, A. Antonov, An approach to the determination of conditions impairing heat transfer under supercritical pressure. *High Temperature* 11 (1973) 529-532.
- [98] Z. Li, D. Zhang, Y. Wu, et al., A new criterion for predicting deterioration of heat transfer to supercritical water in smooth tubes. *Proceedings of the CSEE* 34 (2014) 6304-6309. (in Chinese)
- [99] G.A. Schatte, A. Kohlhepp, C. Wieland, et al., Development of a new empirical correlation for the prediction of the onset of the deterioration of heat transfer to

- supercritical water in vertical tubes. *International Journal of Heat and Mass Transfer* 102 (2016) 133-141.
- [100] S.K. Dubey, K.N. Iyer, R.P. Vedula, et al., Development of a criterion for onset of heat transfer deterioration in supercritical fluid. The 8th International Symposium on Supercritical Water-cooled Reactors (ISSCWR8), Chengdu, China, March 13-15, 2017.
- [101] V.I. Deev, V.S. Kharitonov, A.N. Churkin, Analysis and generalization of experimental data on heat transfer to supercritical pressure water flow in annular channels and rod bundles. *Thermal Engineering* 64 (2017) 142-150.
- [102] K. Goldmann, Heat transfer to supercritical water at 5000 psi flowing at high mass flow rates through round tubes. *International Developments in Heat Transfer, Part III*, ASME, New York, 561-568, 1961.
- [103] E. Abadzic, R.J. Goldstein, Film boiling and free convection heat transfer to carbon dioxide near the critical state. *International Journal of Heat and Mass Transfer* 13 (1970) 1163-1175.
- [104] D. Palko, H. Anglart, Numerical study of heat transfer deterioration. *International Students Workshop on High Performance Light Water Reactors*, Karlsruhe, Germany, March 31-April 3, 2008.
- [105] D. Huang, W. Li, A brief review on the buoyancy criteria for supercritical fluids. *Applied Thermal Engineering* 131 (2018) 977-987.
- [106] G. Zhang, H. Zhang, H.Y. Gu, et al., Experimental and numerical investigation of turbulent convective heat transfer deterioration of supercritical water in vertical tube. *Nuclear Engineering and Design* 248 (2012) 226-237.
- [107] D. Palko, H. Anglart, Theoretical and numerical study of heat transfer deterioration in high performance light water reactor. *Science and Technology of Nuclear Installations* (2008) 1-5.
- [108] Q.L. Wen, H.Y. Gu, Numerical investigation of acceleration effect on heat transfer deterioration phenomenon in supercritical water. *Progress in Nuclear Energy* 53 (2011) 480-486.

- [109] M. Mohseni, M. Bazargan, The effect of the low Reynolds number k- $\epsilon$  turbulence models on simulation of the enhanced and deteriorated convective heat transfer to the supercritical fluid flows. *Heat and Mass Transfer* 47 (2011) 609-619.
- [110] M. Mohseni, M. Bazargan, A new analysis of heat transfer deterioration on basis of turbulent viscosity variations of supercritical fluids. *Journal of Heat Transfer* 134 (12) (2012).
- [111] V.A. Grabezhnaya, P.L. Kirillov, Heat transfer in pipes and rod bundles during flow of supercritical-pressure water. *Atomic Energy* 96 (2004) 358-364.
- [112] V.A. Kurganov, Y.A. Zeigarnik, I.V. Maslakova, Heat transfer and hydraulic resistance of supercritical pressure coolants. Part IV: Problems of generalized heat transfer description, methods of predicting deteriorated heat transfer; empirical correlations; deteriorated heat transfer enhancement; dissolved gas effects. *International Journal of Heat and Mass Transfer* 77 (2014) 1197-1212.
- [113] H. Wang, Q.C. Bi, Z.D. Yang, et al., Experimental and numerical study on the enhanced effect of spiral spacer to heat transfer of supercritical pressure water in vertical annular channels. *Applied Thermal Engineering* 48 (2012) 436-445.
- [114] X.J. Zhu, S. Morooka, Y. Oka, Numerical investigation of grid spacer effect on heat transfer of supercritical water flows in a tight rod bundle. *International Journal of Thermal Sciences* 76 (2014) 245-257.
- [115] X. Zhu, S. Morooka, Y. Oka, Numerical investigation on practicability of reducing MCST by using grid spacer in a tight rod bundle. *Nuclear Engineering and Design* 270 (2014) 198-208.
- [116] V.A. Kurganov, Y.A. Zeigarnik, I.V. Maslakova, Heat transfer and hydraulic resistance of supercritical-pressure coolants. Part I: Specifics of thermophysical properties of supercritical pressure fluids and turbulent heat transfer under heating conditions in round tubes (state of the art). *International Journal of Heat and Mass Transfer* 55 (2012) 3061-3075.

- [117] X. Cheng, B. Kuang, Y.H. Yang, Numerical analysis of heat transfer in supercritical water cooled flow channels. *Nuclear Engineering and Design* 237 (2007) 240-252.
- [118] J. Yang, Y. Oka, Y. Ishiwatari, et al., Numerical investigation of heat transfer in upward flows of supercritical water in circular tubes and tight fuel rod bundles. *Nuclear Engineering and Design* 237 (2007) 420-430.
- [119] Z. Shang, Y. Yao, CFD investigation of heat transfer in supercritical water cooler flow through 3×3 fuel rod bundles. 16th International Conference on Nuclear Engineering (ICONE-16). Orlando, Florida, USA, May 11-15, 2008.
- [120] H.Y. Gu, X. Cheng, Y.H. Yang, CFD analysis of thermal-hydraulic behavior of supercritical water in sub-channels. *Nuclear Engineering and Design* 240 (2010) 364-374.
- [121] F. Mantlik, J. Heina, J. Chervenka, Results of local measurements of hydraulic characteristic in triangular pin bundle. UJV-3778-R, Czech Republic, 1976.
- [122] Z. Shang, S. Lo, Numerical investigation of supercritical water-cooled nuclear reactor in horizontal rod bundles. *Nuclear Engineering and Design* 240 (2010) 776-782.
- [123] X. Yang, G.H. Su, W.X. Tian, et al., Numerical study on flow and heat transfer characteristics in the rod bundle channels under super critical pressure condition. *Annals of Nuclear Energy* 37 (2010) 1723-1734.
- [124] B. Zhang, J.Q. Shan, J. Jiang, Numerical analysis of supercritical water heat transfer in horizontal circular tube. *Progress in Nuclear Energy* 52 (2010) 678-684.
- [125] M. Bazargan, Forced convection heat transfer to turbulent flow of supercritical water in a round horizontal tube. Doctoral dissertation, University of British Columbia, 2001.
- [126] Z. Li, Y. Wu, J. Lu, et al., Heat transfer to supercritical water in circular tubes with circumferentially non-uniform heating. *Applied Thermal Engineering* 70 (2014) 190-200.

- [127] X.L. Lei, H.X. Li, S.Q. Yu, et al., Numerical investigation on the mixed convection and heat transfer of supercritical water in horizontal tubes in the large specific heat region. *Computers and Fluids* 64 (2012) 127-140.
- [128] J. Li, J. Yu, G. Jiang, et al., Assessment of performance of turbulence models of CFX in predicting supercritical water heat transfer in a vertical tube. 20th International Conference on Nuclear Engineering (ICONE-20), Anaheim, California, USA, July 30 - August 3, 2012.
- [129] G. Dutta, R. Maitri, C. Zhang, et al., Numerical models to predict steady and unsteady thermal-hydraulic behaviour of supercritical water flow in circular tubes. *Nuclear Engineering and Design* 289 (2015) 155-165.
- [130] A.P. Ornatskij, S.I. Kalachev, L.F. Glushche, Heat-transfer with rising and falling flows of water in tubes of small diameter at supercritical pressures. *Thermal Engineering* 18 (1971) 137-141.
- [131] A. Churkin, S. Bilbao, K. Yamada, Analysis of the IAEA benchmark exercise on steady state flow in a heated pipe with supercritical water. *Proceedings of the ICAPP*, pp.139-145, 2011.
- [132] K. Podila, Y.F. Rao, CFD analysis of flow and heat transfer in Canadian supercritical water reactor bundle. *Annals of Nuclear Energy* 75 (2015) 1-10.
- [133] J.B. Xiong, X. Cheng, Y.H. Yang, Numerical analysis on supercritical water heat transfer in a 2x2 rod bundle. *Annals of Nuclear Energy* 80 (2015) 123-134.
- [134] K. Podila, Y.F. Rao, CFD modelling of supercritical water flow and heat transfer in a 2x2 fuel rod bundle. *Nuclear Engineering and Design* 301 (2016) 279-289.
- [135] H. Wang, Q.C. Bi, L.C. Wang, et al., Heat transfer characteristics of supercritical water in a 2x2 rod bundle - numerical simulation and experimental validation. *Applied Thermal Engineering* 100 (2016) 730-743.
- [136] A. Zvorykin, S. Aleshko, N. Fialko, et al., Computer simulation of flow and heat transfer in bare tubes at supercritical parameters. 24th International Conference on Nuclear Engineering (ICONE-24), Charlotte, North Carolina, USA, June 26-30, 2016.

- [137] P. Kirillov, R. Pometko, A. Smirnov, et al., Experimental study on heat transfer to supercritical water flowing in 1-and 4-m-long vertical tubes. Proceedings of the GLOBAL'05, Tsukuba, Japan, 2005.
- [138] Z. Gao, J. Bai, Numerical analysis on nonuniform heat transfer of supercritical pressure water in horizontal circular tube. *Applied Thermal Engineering* 120 (2017) 10-18.
- [139] M.K. Rowinski, J. Zhao, T.J. White, et al., Numerical investigation of supercritical water flow in a vertical pipe under axially non-uniform heat flux. *Progress in Nuclear Energy* 97 (2017) 11-25.
- [140] A.P. Ornatsky, L.F. Glushchenko, E.T. Siomin, et al., The research of temperature conditions of small diameter parallel tubes cooled by water under supercritical pressures. 4th International Heat Transfer Conference, Paris, Versailles, France, 1970.
- [141] X. Zhu, X. Du, Y. Ding, et al., Analysis of entropy generation behavior of supercritical water flow in a hexagon rod bundle. *International Journal of Heat and Mass Transfer* 114 (2017) 20-30.
- [142] X. Zhu, X. Du, Q. Li, et al., Study on the effects of system parameters on entropy generation behavior of supercritical water in a hexagon rod bundle. *International Journal of Heat and Mass Transfer* 117 (2018) 669-681.
- [143] B.E. Launder, D.B. Spalding, The numerical computation of turbulent flows. *Computer Methods in Applied Mechanics and Engineering* 103 (1974) 269-289.
- [144] V. Yakhot, S.A. Orszag, S. Thangam, et al., Development of turbulence models for shear flows by a double expansion technique. *Physics of Fluids A* 4 (1992) 1510-1520.
- [145] S.H. Kim, Y.I. Kim, Y.Y. Bae, et al., Numerical simulation of the vertical upward flow of water in a heated tube at supercritical pressure, Proceedings of the International Congress on Advances in Nuclear Power Plants (ICAPP'04), Pittsburgh, PA, USA, 2004.

- [146] K. Rehme, The structure of turbulence in rod bundles and the implications on natural mixing between the subchannels. *International Journal of Heat and Mass Transfer* 35 (1992) 567-581.
- [147] M.T. Kao, M. Lee, Y.M. Ferng, Heat transfer deterioration in a supercritical water channel. *Nuclear engineering and design* 240 (2010), 3321-3328.
- [148] M. Bazargan, M. Mohseni, Algebraic zero-equation versus complex two-equation turbulence modeling in supercritical fluid flows. *Computers and Fluids* 60 (2012) 49-57.
- [149] Y. Zhang, C. Zhang, J. Jiang, Numerical simulation of heat transfer of supercritical fluids in circular tubes using different turbulence models. *Journal of Nuclear Science and Technology* 48 (2011) 366-373.
- [150] A. Kiss, A. Aszodi, Numerical investigation on the physical background of deteriorated heat transfer mode in supercritical pressure water. In *Proceedings of the 6th International Symposium on Supercritical Water-Cooled Reactors (ISSCWR-6)*, Shenzhen, China, March 3-7, 2013.
- [151] E. Laurien, Numerical simulation of flow and heat transfer of fluids at supercritical pressure. *Proceedings of the CFD for Nuclear Reactor Safety Applications (CFD4NRS-3) Workshop*, Bethesda, Maryland, USA, 2010.
- [152] T. Wei, W.W. Willmarth, Reynolds-number effects on the structure of a turbulent channel flow. *Journal of Fluid Mechanics* 204 (1989) 57-95.
- [153] M. Sharabi, W. Ambrosini, Discussion of heat transfer phenomena in fluids at supercritical pressure with the aid of CFD models. *Annals of Nuclear Energy* 36 (2009) 60-71.
- [154] J.Y. Yoo, The turbulent flows of supercritical fluids with heat transfer. *Annual Review of Fluid Mechanics* 45 (2013) 495-525.
- [155] J.K. Kim, H.K. Jeon, J.Y. Yoo, et al., Experimental study on heat transfer characteristics of turbulent supercritical flow in vertical circular/non-circular tubes. *Proceedings of the 11th International Topical Meeting on Nuclear Reactor Thermal Hydraulics (NURETH-11)*, Avignon, France, October 2-6, 2005.

- [156] Q.L. Wen, H.Y. Gu, Numerical simulation of heat transfer deterioration phenomenon in supercritical water through vertical tube. *Annals of Nuclear Energy* 37 (2010) 1272-1280.
- [157] Y.Y. Bae, H.Y. Kim, Convective heat transfer to CO<sub>2</sub> at a supercritical pressure flowing vertically upward in tubes and an annular channel. *Experimental Thermal and Fluid Science* 33 (2009) 329-339.
- [158] M. Jaromin, H. Anglart, A numerical study of heat transfer to supercritical water flowing upward in vertical tubes under normal and deteriorated conditions. *Nuclear Engineering and Design* 264 (2013) 61-70.
- [159] X.L. Lei, H.X. Li, Y.Q. Zhang, et al., Effect of buoyancy on the mechanism of heat transfer deterioration of supercritical water in horizontal tubes. *Journal of Heat Transfer* 135(7) (2013).
- [160] S.Q. Yu, H.X. Li, X.L. Lei, et al., A Comparison of heat transfer characteristics of supercritical pressure water flow in different arrangement experimental tubes. *Proceedings of the 5th International Symposium on Supercritical Water-Cooled Reactors (ISSCWR-5)*, Vancouver, BC, Canada, March 13-16, 2011.
- [161] L. Liu, Z. Xiao, X. Yan, et al., Numerical simulation of heat transfer deterioration phenomenon to supercritical water in annular channel. *Annals of Nuclear Energy* 53 (2013) 170-181.
- [162] L.F. Glushchenko, O. Gandziuk, Temperature conditions at the wall of an annular channel with internal heating at supercritical pressures. *High Temperature* 10 (1973) 734-738.
- [163] P. Bradshaw, Possible origin of Prandtl's mixing-length theory. *Nature* 249 (1974) 135-136.
- [164] T. Schulenberg, D.C. Visser, Thermal-hydraulics and safety concepts of supercritical water cooled reactors. *Nuclear Engineering and Design* 264 (2013) 231-237.
- [165] F. Menter, Zonal two equation  $k-\omega$  turbulence models for aerodynamic flows. *Proceedings of the 23rd Fluid Dynamics, Plasmadynamics and Lasers Conference*. 1993, 2906.

- [166] Y. Zhu, Numerical investigation of the flow and heat transfer within the core cooling channel of a supercritical water reactor. University of Stuttgart - Universitätsbibliothek, 2010.
- [167] C.J. Geankoplis, Transport Processes and Separation Process Principles. 167 (2003) 287-302.
- [168] F.G. Schmitt, About Boussinesq's turbulent viscosity hypothesis: historical remarks and a direct evaluation of its validity. *Comptes Rendus Mécanique* 335 (2007) 617-627.
- [169] M. Bazargan, D. Fraser, Heat transfer to supercritical water in a horizontal pipe: modeling, new empirical correlation, and comparison against experimental data. *Journal of Heat Transfer* 131(6) (2009).
- [170] M. Mohseni, M. Bazargan, Effect of turbulent Prandtl number on convective heat transfer to turbulent flow of a supercritical fluid in a vertical round tube. *Journal of Heat Transfer* 133(7) (2011).
- [171] Y.Y. Bae, A new formulation of variable turbulent Prandtl number for heat transfer to supercritical fluids. *International Journal of Heat and Mass Transfer* 92 (2016) 792-806.
- [172] R. Tian, D.B. Wang, X.Y. Dai, et al., Investigation of a variable turbulent Prandtl number model for the heat transfer to supercritical fluids. The 8th International Symposium on Supercritical Water-cooled Reactors (ISSCWR8), Chengdu, China, March 13-15, 2017.
- [173] R.B. Hasan, Turbulent Prandtl number and its use in prediction of heat transfer coefficient for liquids. *Nahrain University, College of Engineering Journal* 10 (2007) 53-64.
- [174] M. Mohseni, M. Bazargan, A new correlation for the turbulent Prandtl number in upward rounded tubes in supercritical fluid flows. *Journal of Heat Transfer* 138(8) (2016).
- [175] Y.Y. Bae, Mixed convection heat transfer to carbon dioxide flowing upward and downward in a vertical tube and an annular channel. *Nuclear Engineering and Design* 241 (2011) 3164-3177.

- [176] H. Mori, M. Ohno, K. Ohishi, Heat transfer to a supercritical pressure fluid flowing in a sub-bundle channel. 16th Pacific Basin Nuclear Conference, Aomori, Japan, October 13-18, 2008.
- [177] H. Zahlan, D. Groeneveld, S. Tavoularis, Measurements of convective heat transfer to vertical upward flows of CO<sub>2</sub> in circular tubes at near-critical and supercritical pressures. *Nuclear Engineering and Design* 289 (2015) 92-107.
- [178] F. Feuerstein, A.C. Silva, D. Klingel, Large-scale heat transfer experiments with supercritical R134a flowing upward in a circular tube. The 47th Annual Meeting on Nuclear Technology, 2016.
- [179] A. Pucciarelli, W. Ambrosini, Improvements in the prediction of heat transfer to supercritical pressure fluids by the use of algebraic heat flux models. *Annals of Nuclear Energy* 99 (2017) 58-67.
- [180] B. Deng, W. Wu, S. Xi, A near-wall two-equation heat transfer model for wall turbulent flows. *International Journal of Heat and Mass Transfer* 44 (2001) 691-698.
- [181] S. Kenjereš, S.B. Gunarjo, K. Hanjalić, Contribution to elliptic relaxation modelling of turbulent natural and mixed convection. *International Journal of Heat and Fluid Flow* 26 (2005) 569-586.
- [182] X.Y. Xu, T. Ma, M. Zeng, Numerical study of the effects of different buoyancy models on supercritical flow and heat transfer. In ASME 2013 Heat Transfer Summer Conference, Minneapolis, MN, USA, July 14-19, 2013.
- [183] V. Papp, A. Pucciarelli, M. Sharabi, Use of algebraic heat flux models to improve heat transfer predictions for supercritical pressure fluids. In 24th International Conference on Nuclear Engineering (ICONE-24), Charlotte, North Carolina, USA, June 26-30, 2016.
- [184] J.B. Xiong, X. Cheng, Turbulence modelling for supercritical pressure heat transfer in upward tube flow. *Nuclear Engineering and Design* 270 (2014) 249-258.
- [185] J.H. Bae, J.Y. Yoo, H. Choi, Direct numerical simulation of turbulent supercritical flows with heat transfer. *Physics of fluids* 17 (2005) 105104.

- [186] A. Pucciarelli, I. Borroni, M. Sharabi, Results of 4-equation turbulence models in the prediction of heat transfer to supercritical pressure fluids. *Nuclear Engineering and Design* 281 (2015) 5-14.
- [187] A. Pucciarelli, M. Sharabi, W. Ambrosini, Prediction of heat transfer to supercritical fluids by the use of Algebraic Heat Flux Models. *Nuclear Engineering and Design* 297 (2016) 257-266.
- [188] J. Fewster, Mixed forced and free convective heat transfer to supercritical pressure fluids flowing in vertical pipes (PhD thesis). University of Manchester, 1976.
- [189] M.J. Watts, Heat transfer to supercritical pressure water - mixed convection with upflow and downflow in a vertical tube (PhD thesis). University of Manchester, 1980.
- [190] P. Sagaut, *Large Eddy Simulation for Incompressible Flows - An Introduction*. Springer, 2001.
- [191] B. Ničeno, M. Sharabi, Large eddy simulation of turbulent heat transfer at supercritical pressures. *Nuclear Engineering and Design* 261 (2013) 44-55.
- [192] W. Jäger, V.H.S. Espinoza, A. Hurtado, Review and proposal for heat transfer predictions at supercritical water conditions using existing correlations and experiments. *Nuclear Engineering and Design* 241 (2011) 2184-2203.
- [193] X. Liu, B. Kuang, Wide-ranged heat transfer correlations of supercritical water in vertical upward channels. *Chinese Journal of Nuclear Science and Engineering* 32(4) (2012), 344-353.
- [194] W. Chen, X. Fang, A new heat transfer correlation for supercritical water flowing in vertical tubes. *International Journal of Heat and Mass Transfer* 78 (2014) 156-160.
- [195] H. Wang, Q.C. Bi, L.C. Wang, Nonuniform heat transfer of supercritical water in a tight rod bundle - Assessment of correlations. *Annals of Nuclear Energy* 110 (2017) 570-583.
- [196] S. Mokry, I. Pioro, Investigation of characteristic-temperature approaches for heat-transfer correlations at supercritical conditions. In *21st International*

Conference on Nuclear Engineering (ICONE-21). Chengdu, China, July 29 - August 2, 2013.

### Figure and table captions

Table 1 Experimental studies on heat transfer of SCW in tubes.

Table 2 Experimental studies on heat transfer of SCW in annuli and rod-bundles.

Table 3 Selected correlations in predicting the onset of HTD.

Table 4 Numerical simulations on heat transfer of SCW.

Table 5 Numerical investigations on HTD of SCW.

Table 6 Prediction models of the turbulent Prandtl number.

Table 7 Recently developed heat-transfer correlations for SCW.

Figure 1. Pressure-Temperature diagram of water.

Figure 2. Thermophysical properties of SCW calculated from the NIST database [15].

Figure 3. Enhanced and deteriorated heat transfer at supercritical pressures.

Figure 4. Circumferential wall temperature distributions in 2×2 bare-rod bundles (a) Wang et al. [66]; (b) Gu et al. [68].

Figure 5. Heat transfer deterioration in vertical and horizontal tubes.

Figure 6. Comparison of the predicted heat flux with the experimental data.

Figure 7. Typical velocity profiles near the wall.

Figure 8. Comparison between the predicted and experimental wall temperatures at a low mass flux of  $430 \text{ kg/m}^2\text{s}$  [89].

Figure 9. Comparison between the predicted and experimental wall temperatures at a high mass flux of  $1500 \text{ kg/m}^2\text{s}$  [107].

Figure 10. Comparison of the measured and predicted wall temperatures with different turbulent Prandtl numbers.

Figure 11. Comparisons of the wall temperature using the dynamic definition of  $C_{t4}$  with experimental data.

ACCEPTED MANUSCRIPT

Table 1

Authors	Flow direction	Experimental conditions	Main findings
Bazargan et al. [27]	Horizontal	$P=23-27$ MPa; $G=330-1230$ kg/m <sup>2</sup> s; $q=0-330$ kW/m <sup>2</sup> ; $d=6.3$ mm; $L=3$ m.	(a) Non-uniform wall temperatures in horizontal flow are mainly caused by buoyancy (b) Buoyancy criteria proposed for vertical tubes are not applicable to horizontal tubes (c) Petukhov et al. [28] criterion for negligible buoyancy is recommended
Kirillov and Grabezhnaya [26]	Vertically upward	$P=23-25$ MPa; $G=200-2000$ kg/m <sup>2</sup> s; $q=400-1200$ kW/m <sup>2</sup> ; $t_{in}=320-380$ °C; $d=10$ mm; $L=4$ m; roughness 0.63-0.8 μm.	(a) Correlation of Bishop et al. [23] can be used for preliminary calculations (b) A lower boundary for DHT considering molar weight of fluids was proposed
Pis'menny et al. [29, 30]	Vertically upward and downward	$P=23.5$ MPa; $G=250-2200$ kg/m <sup>2</sup> s; $q=360-3210$ kW/m <sup>2</sup> ; $t_{in}=100-415$ °C; $d=6.28, 9.5$ mm; $L=0.36-0.6$ m; roughness 0.25-0.5 μm	(a) Free convection decreases the heat transfer coefficient in upward flow (b) DHT starts earlier in the upward flow compared to that in the downward flow (c) Petukhov et al. [31] correlation best predicts the heat transfer in upward and downward flows
Yin et al. [32]	Inclined, angle of 20°	$P=23-30$ MPa; $G=600-1200$ kg/m <sup>2</sup> s; $q=200-600$ kW/m <sup>2</sup> ; $d=26$ mm; $L=2$ m.	(a) Non-uniform heat transfer exists along the circumference of the inclined tube (b) Wall temperatures at the top are higher than those at the bottom due to buoyancy (c) DHT is weakened with increasing mass velocity or pressure
Zhu et al. [33]	Vertically upward	$P=9-30$ MPa; $G=600-1200$ kg/m <sup>2</sup> s; $q=200-600$ kW/m <sup>2</sup> ; $d=26$ mm; $L=1$ m.	(a) The increase of pressure weakens both the heat transfer enhancement and deterioration (b) The degree of HTD is reduced when fluid enthalpy is far from the pseudo-critical point

(c) Swenson et al. [24] correlation best fits the experimental data

Mokry et al. [34, 35]	Vertically upward	$P=24$ MPa; $G=200-1500$ kg/m <sup>2</sup> s; $q=70-1250$ kW/m <sup>2</sup> ; $t_{in}=320-350$ °C; $d=10$ mm; $L=4$ m; roughness 0.63-0.8 μm.	(a) There are three heat-transfer regimes at supercritical pressures (b) The appearance and magnitude of enhancement and deterioration are affected by $P$ , $G$ , $q$ and $t_b$ (c) A new heat-transfer correlation was developed using the method of dimensional analysis
Yu et al. [36]	Horizontal	$P=23-25$ MPa; $G=300-700$ kg/m <sup>2</sup> s; $q=200-400$ kW/m <sup>2</sup> ; $H_b=1000-3000$ kJ/kg; $d=26$ mm; $L=2$ m.	(a) Buoyancy leads to non-uniform wall temperature and heat flux distributions in horizontal flows (b) At DHT conditions, the increase in wall temperature is more severe in vertical upward tube (c) Smaller diameter helps to reduce buoyancy effect in horizontal flows
Yu et al. [37]	Horizontal	$P=25$ MPa; $G=300-1000$ kg/m <sup>2</sup> s; $q=50-400$ kW/m <sup>2</sup> ; $d=26, 43$ mm; $L=2$ m.	(a) DHT induced by buoyancy occurs when $q/G > 0.5$ (b) The effects of tube diameter on heat transfer are noticeable at high $q/G$ condition (c) Both criteria of Jackson and Hall [38] and Petukhov and Polyakov [39] are able to predict the onset of buoyancy at DHT regime
Shen et al. [40]	Vertically downward	$P=11.5-28$ MPa; $G=450-1536$ kg/m <sup>2</sup> s; $q=50-585$ kW/m <sup>2</sup> ; $d=17$ mm; $L=2$ m.	(a) Heat transfer in high enthalpy region is much better than that in low enthalpy region (b) Far from the pseudo-critical point, heat transfer in downward flow is superior to upward flow
Zhao et al. [41]	Vertically downward	$P=23-26$ MPa; $G=450-1500$ kg/m <sup>2</sup> s; $q=190-1400$ kW/m <sup>2</sup> ; $t_{in}=240-350$ °C; $t_b=280-400$ °C; $d=7.6$ mm; $L=2.64$ m.	(a) Mass flux has great effects on heat transfer, while the effects of pressure are negligible (b) Heat transfer in upward flow is better than that in downward flow at low heat

fluxes, but the case is opposite at high heat fluxes

(c) Cheng et al. [42] correlation shows best agreement with the experimental data

Gu et al. [43]	Vertically upward	$P=23-26$ MPa; $G=450-1500$ kg/m <sup>2</sup> s; $q=190-1400$ kW/m <sup>2</sup> ; $t_b=280-460$ °C; (1) $d=7.6$ mm, $L=2.64$ m; (2) $d=10$ mm, $L=2.5$ m.	(a) Entrance effect could exist over a much larger region than expected (b) The effects of tube diameter are inversed within and outside the pseudo-critical region (c) Correlations of Jackson [44] and Cheng et al. [42] show good agreements with test data
Lei et al. [45]	Horizontal; Vertically upward	$P=23-28$ MPa; $G=200-600$ kg/m <sup>2</sup> s; $q=100-400$ kW/m <sup>2</sup> ; $d=26$ mm; $L=2$ m.	(a) Wall temperature profiles are different for vertical and horizontal tubes at DHT regime (b) At the same parameters, buoyancy in horizontal flows is stronger than that of vertical flows (c) The criteria of buoyancy and thermal acceleration proposed by Petukhov and Polyakov [39] are superior to other criteria for tube flows
Shen et al. [46]	Vertically upward	$P=11-32$ MPa; $G=170-800$ kg/m <sup>2</sup> s; $q=85-505$ kW/m <sup>2</sup> ; $d=19$ mm; $L=2$ m.	(a) Acceleration number derived by Cheng et al. [42] is appropriate to predict heat transfer (b) Correlations of Mokry et al. [35] and Bishop et al. [23] predict the closest to experimental heat transfer coefficients

Table 2

Authors	Geometries	Experimental conditions	Main findings
Licht et al. [55]	Circular annular; square annular	$P=25$ MPa; $G=350-1425$ kg/m <sup>2</sup> s; $q=125-1000$ kW/m <sup>2</sup> ; $t_{in}=300-400$ °C; $d_{rod}=10.7$ mm; circular annular gap 16.1 mm; square annular gap 9.05 mm; $L=3.3$ m; grid spacer; upward flow.	(a) HTD depends on flow geometry and hydraulic diameter (b) At normal heat transfer conditions, circular annulus has a similar performance with tubes (c) Heat transfer data agree closely with the Jackson correlation [56] (d) The onset of buoyancy aligns with criteria proposed in Jackson [38] and Seo et al. [57]
Razumovskiy et al. [58-60]	Circular annular; 3-rod bundle; 7-rod bundle	Annular: $P=22.6, 24.5$ MPa; $G=800-3000$ kg/m <sup>2</sup> s; $q=1030-3450$ kW/m <sup>2</sup> . 3-rod bundle: $P=22.6, 24.5, 27.5$ MPa; $G=1000-2700$ kg/m <sup>2</sup> s; $q=1250-4580$ kW/m <sup>2</sup> . 7-rod bundle: $P=22.6, 24.5, 27.5$ MPa; $G=700-1500$ kg/m <sup>2</sup> s; $q=500-1600$ kW/m <sup>2</sup> . $d_{rod}=5.2$ mm; $L=485$ mm; upward flow.	(a) HTD was observed in all three test sections (b) During HTD, the peak of wall temperature appeared near the outlet first and moved to the inlet direction with increasing heat flux (c) Pressure appears to have little effect on heat transfer (d) Pressure oscillation was not observed in the experiments even at DHT conditions
Li et al. [61]	Square annular	$P=23-25$ MPa; $G=500-1200$ kg/m <sup>2</sup> s; $q=200-800$ kW/m <sup>2</sup> ; $t_{in}=300-400$ °C; $d_{rod}=10$ mm; gap of 2.5 mm; $L=1.5$ m; wire-wrapped spacer, pitch of 200 mm; upward flow.	(a) Spacers do not enhance heat transfer significantly at the normal heat-transfer regime (b) The Jackson criterion [38] is capable in predicting buoyancy and the onset of HTD (c) Pressure pulsation and temperature oscillation were observed when $t_b$ approaching $t_{pc}$
Gang et al. [62]	Circular annular	$P=23-28$ MPa; $G=350-1000$ kg/m <sup>2</sup> s; $q=200-1000$ kW/m <sup>2</sup> ; $t_{in}$ up to 400 °C; $d_{rod}=8$ mm; gaps of 4 mm, 6 mm; $L=1.4$ m;	(a) DHT is more severe in the annular channel with a 4-mm gap than a 6-mm gap (b) The effect of pressure on wall temperature are noticeable in all heat

		wire-wrapped spacer, pitch of 50 mm; transfer regimes upward flow.	(c) Wire-wrapped spacer enhances downstream heat transfer, especially at high mass fluxes (d) Experimental Nusselt numbers agree closely with the Jackson correlation [44]
Yang et al. [63]	Circular annular	$P=23-25$ MPa; $G=700-1000$ kg/m <sup>2</sup> s; $q=200-1000$ kW/m <sup>2</sup> ; $d_{rod}=8$ mm; gap of 2 mm; $L=620$ mm; grid spacer; upward and downward flows.	(a) Heat transfer coefficients for downward flow are higher than those for upward flow, particularly at high $q/G$ cases (b) The effect of spacer on heat transfer depends strongly on mass flux (c) Experimental Nusselt numbers agree closely with the correlation of Swenson et al. [24]
Li et al. [64]; Zhao et al. [65]	Circular annular; 2×2 rod bundle	$P=23-26$ MPa; $G=432-1775$ kg/m <sup>2</sup> s; $q=189-1498$ kW/m <sup>2</sup> ; $t_{in}=264-357$ °C; upward flow. Annular: $d_{rod}=8$ mm; gap of 2.4 mm; $L=2640$ mm. 2×2 rod bundle: $d_{rod}=8$ mm; $P/D=1.18, 1.3$ ; $L=1328$ mm; grid spacer.	(a) Non-uniform wall temperature in rod circumference was observed in the bundle (b) Slight HTD was observed in bundle with $P/D$ of 1.18 but not with $P/D$ of 1.3 (c) Grid spacer enhances local heat transfer significantly but decays shortly downstream. (d) Heat transfer in the 2×2 rod bundle is improved compared to tubes or annuli (based on cross-sectional averaged flow conditions).
Wang et al. [66]	2×2 rod bundle	$P=23-28$ MPa; $G=350-1000$ kg/m <sup>2</sup> s; $q=200-1000$ kW/m <sup>2</sup> ; $t_{in}=200-450$ °C; $d_{rod}=8$ mm; $P/D=1.18$ ; $L=600$ mm; grid spacer; upward flow.	(a) Non-uniform wall temperature was observed along the circumference of the rods (b) Circumferential wall temperature gradient is the smallest at $t_{pc}$ (c) Effects of pressure, heat flux and mass flux on heat transfer in the 2×2 rod bundle are similar to those observed in tubes (d) Experimental Nusselt numbers agree closely with the Jackson correlation

Gu et al. [67, 68]	2×2 bundle	rod $P=23-26$ MPa; $G=400-1200$ kg/m <sup>2</sup> s; $q=300-1000$ kW/m <sup>2</sup> ; $t_b=200-480$ °C; $d_{rod}=10$ mm; $P/D=1.18$ ; $L=833$ mm; grid spacer; upward flow.	[44] (a) Non-uniform wall-temperature distributions are attributed to the change in the subchannel flow-area around the heated rod (b) High wall temperatures were observed at the surface facing the corner subchannel and low wall temperature at the surface facing the central subchannel (c) Correlations of Bishop et al. [23] and Jackson and Fewster [69] predict closely the experimental Nusselt numbers (d) HTD was not observed during mass flux or power transients
Gu et al. [70]	2×2 bundle	rod $P=23-26$ MPa; $G=400-1400$ kg/m <sup>2</sup> s; $q=300-1000$ kW/m <sup>2</sup> ; $t_b=280-500$ °C; $d_{rod}=10$ mm; $P/D=1.18$ ; $L=750$ mm; wire-wrapped spacer, pitch of 250 mm; upward flow.	(a) Effects of system parameters on heat transfer are similar to those in bare bundles (b) Non-uniform wall-temperature distributions were observed around the heated rod (c) Wire-wrapped spacers appear to be able to suppress, but not eliminate, the occurrence of HTD in the 2×2 rod bundle (d) Correlations of Bishop et al. [23] and Jackson and Fewster [69] predict closely the experimental Nusselt numbers
Wang et al. [71]	2×2 bundle	rod $P=23-28$ MPa; $G=400-1000$ kg/m <sup>2</sup> s; $q=200-1000$ kW/m <sup>2</sup> ; $t_{in}=200-450$ °C; $d_{rod}=8$ mm; $P/D=1.18$ ; $L=600$ mm; wire-wrapped spacer, pitch of 200 mm; upward flow.	(a) Non-uniform circumferential wall-temperature was observed around the heated rod with the peak at the surface facing the corner subchannel (b) A localized wall-temperature peak was also noticed at the spacer location (b) The wire-wrapped spacers enhance heat transfer, particularly near the $H_{pc}$ , compared to the bare rod bundle (c) Correlations of Jackson [44] and Krasnoshchekov et al. [72] predict closely the experimental Nusselt numbers

Zhao et al. [73] Circular annular  $P=15.5-26$  MPa;  $G=500-1600$  kg/m<sup>2</sup>s;  $q=450-1400$  kW/m<sup>2</sup>;  $t_b=310-390$  °C;  $d_{rod}=8$  mm; gap of 3.65 mm;  $L=2032$  mm; grid spacer; upward flow.

(a) The grid spacer enhances heat transfer but the enhancement decays exponentially to the downstream

(b) The effect of spacer on heat transfer are negligible small after 40 times of  $D_{hy}$

(c) A new correlation was proposed to predict the local enhancement in heat transfer due to spacers

---

Table 3

Authors	Correlations
Styrikovich et al. [92]	$q = 0.58G$
Vikhrev et al. [93]	$q = 0.4G$
Lokshin et al. [94]	$q = 0.7G$
Kondrat'ev [95]	$q = 5.815 \times 10^{-17} Re_b^{1.7} \left( \frac{P}{1.01325} \right)^{4.5}$
Ogata and Sato [96]	$q = 0.034 \cdot \sqrt{\frac{f}{8}} \cdot \left( \frac{c_p}{\beta} \right)_{pc} \cdot G$
Yamagata et al. [19]	$q = 0.2G^{1.2}$
Protopopov et al. [97]	$q = G \frac{1.3}{(t_{pc} - t_b) c_{pb} (f/8) (v_w/v_{pc})^{1.3}}$
Jackson and Hall [38]	$\frac{q}{\rho_b G} \cdot \left( \frac{\partial \rho}{\partial h} \right)_{P,b} \left( \frac{\mu_w}{\mu_b} \right) \left( \frac{\rho_w}{\rho_b} \right)^{-0.5} \frac{1}{Re_b^{0.7}} \geq C$
Petukhov et al. [31]	$q = 0.1875 \cdot f \cdot \left( \frac{c_p}{\beta} \right)_{pc} \cdot G$
Cheng et al. [42]	$q = 1.354 \times 10^{-3} \left( \frac{c_p}{\beta} \right)_{pc} \cdot G$
Mokry et al. [35]	$q = -58.97 + 0.745G$
Li et al. [98]	$q = d \cdot \left( \frac{0.36G}{d} - 1.1 \right)^{1.21}$
Schatte et al. [99]	$q = 1.942 \times 10^{-6} \cdot G^{0.795} \cdot (30 - d)^{0.339} \cdot \left( \frac{c_p}{\beta} \right)_{pc}^{2.065}$
Dubey et al. [100]	$ND_{om} = \left( \frac{q \mu_{pc}}{G Pr_{pc}^{0.5} \lambda_{pc} \Delta T_0} \right) \left( \frac{c_{pc}}{c_{pc^*}} \right)^{0.55} \leq 2 \times 10^{-4}$
Deev et al. [101]	$q = 5.32 \cdot G^{1.265} \cdot d^{0.865}$

Table 4

Authors	CFD code	Assessed turbulence model	Flow geometry	Dimension	Benchmark data	Recommended turbulence model
Seo et al. [57]	FLUENT	Standard $k-\varepsilon$ model	Vertical tubes	2D	Yamagata et al. [19], Shitsman [22]	-
Cheng et al. [117]	CFX 5.6	$\varepsilon$ type: Standard $k-\varepsilon$ , RNG $k-\varepsilon$ , Reynolds stress models of SSG and LRR; $\omega$ type: SST $k-\omega$ , Reynolds stress- $\omega$ model (RSO)	Vertical tube and sub-channels	3D	Yamagata et al. [19]	SSG Reynolds stress model
Yang et al. [118]	STAR-CD 3.24	Standard $k-\varepsilon$ high- $Re$ , Standard $k-\varepsilon$ low- $Re$ , V2F, RNG $k-\varepsilon$ , Chen $k-\varepsilon$ , Speziale $k-\varepsilon$ , Two-layer models, Standard $k-\omega$ high- $Re$ , SST $k-\omega$ high- $Re$ , Standard $k-\omega$ low- $Re$ , SST $k-\omega$ low- $Re$	Vertical tube and sub-channels	3D	Yamagata et al. [19]	Two-layer model (Hassid and Poreh)
Shang and Yao [119]	STAR-CD 4.02	Speziale quadratic high- $Re$ $k-\varepsilon$ model, Standard high- $Re$ $k-\varepsilon$ model	Vertical 3x3 rod bundle	3D	-	Speziale quadratic high- $Re$ $k-\varepsilon$ model
Licht et al. [74]	FLUENT 6.3.26	Reynolds stress model	Vertical annulus	3D	Licht et al. [55, 74]	-
Shang [88]	STAR-CD 4.02	Speziale quadratic high- $Re$ $k-\varepsilon$ model	Vertical tube and rod bundles	3D	Yamagata et al. [19]	-
Gu et al. [120]	CFX 5.6	$\varepsilon$ type: Standard $k-\varepsilon$ , SSG Reynolds stress model; $\omega$ type: SST $k-\omega$ , RSO Reynolds stress- $\omega$ model	Vertical sub-channels	3D	Mantlik et al. [121]	SSG Reynolds stress model

Shang and Lo [122]	STAR-CD 4.02	Speziale quadratic high- $Re$ $k$ - $\varepsilon$ model	Horizontal rod bundles	3D	-	-
Yang et al. [123]	CFX	Standard $k$ - $\varepsilon$ , RNG $k$ - $\varepsilon$ , Modified RNG $k$ - $\varepsilon$	Vertical rod bundle	3D	Yamagata et al. [19]	Modified RNG $k$ - $\varepsilon$ model
Zhang et al. [124]	Unstated	Standard $k$ - $\varepsilon$ , RNG $k$ - $\varepsilon$ , Realizable $k$ - $\varepsilon$	Horizontal tube	3D	Yamagata et al. [19], Bazargan [125]	Standard $k$ - $\varepsilon$ model
Li et al. [126]	FLUENT	SST $k$ - $\omega$ model	Vertical tubes	3D	Ackerman [82], Zhu et al. [33]	-
Shang and Chen [80]	STAR-CD	Speziale non-linear high- $Re$ $k$ - $\varepsilon$ model	Horizontal tubes	3D	Bazargan et al. [27]	-
Lei et al. [127]	FLUENT	RNG $k$ - $\varepsilon$ model	Vertical and horizontal tubes	3D	Yamagata et al. [19], Swenson et al. [24]	-
Li et al. [128]	CFX	$\varepsilon$ type: Standard $k$ - $\varepsilon$ , RNG $k$ - $\varepsilon$ , Reynolds stress models of LRR, QI and SSG, Algebraic Reynolds stress EARSMS; $\omega$ type: Standard $k$ - $\omega$ , SST $k$ - $\omega$ , BSL $k$ - $\omega$ , Reynolds stress models of BSL-RSM, ROS, Algebraic Reynolds stress BSL-EARSMS	Vertical tubes	3D	Yamagata et al. [19], Pis'menny et al. [30]	BSL-EARSMS for high $G$ , none for HTD
Wang et al. [113]	FLUENT	Standard $k$ - $\varepsilon$ , RNG $k$ - $\varepsilon$ , Realizable $k$ - $\varepsilon$	Vertical annulus	3D	Gang et al. [62], Wang et al. [113]	RNG $k$ - $\varepsilon$ model
Zhu et al. [114]	STAR CCM+ 6.04	Standard high- $Re$ $k$ - $\varepsilon$ , Standard low- $Re$ $k$ - $\varepsilon$ , Realizable high- $Re$ $k$ - $\varepsilon$ , Standard two-layer $k$ - $\varepsilon$ models of WO and NR	Vertical sub-channels	3D	Empirical correlations	Standard two layer $k$ - $\varepsilon$ model of Wolfstein (WO)

Dutta et al. [129]	FLUENT 14.5, THRUST (in-house code)	SST $k-\omega$ model, Reynolds stress model, 1-D TH model	Vertical tubes	2D and 1D	Ornatskij et al. [130], Mokry et al. [35], Churkin et al. [131]	-
Podila and Rao [132]	STAR CCM+ 7.04	Low- $Re$ SST $k-\omega$ model	Vertical sub-channels	3D	-	-
Xiong et al. [133]	CFX 5.6	SSG Reynolds stress model, $\omega$ -RSM model, BSL-RSM model	Vertical rod bundle	2x2 3D	Zhao et al. [65]	-
Podila and Rao [134]	STAR CCM+ 9.02	SST $k-\omega$ model, Low- $Re$ V2F model	Vertical rod bundles	2x2 3D	Wang et al. [66], Wang et al. [71]	-
Wang et al. [135]	CFX	RNG $k-\varepsilon$ , SST $k-\omega$ , SSG Reynolds stress model	Vertical rod bundle	2x2 3D	Wang et al. [66]	SSG Reynolds stress model
Zvorykin et al. [136]	FLUENT	Standard $k-\varepsilon$ , Realizable $k-\varepsilon$ , Low- $Re$ models of AKN and LB, SST $k-\omega$ , BSL $k-\omega$	Vertical tube	2D	Kirillov et al. [137]	SST $k-\omega$ model
Gao and Bai [138]	FLUENT	RNG $k-\varepsilon$ model	Horizontal tubes	3D	Yamagata et al. [19]	-
Rowinski et al. [139]	FLUENT	SST $k-\omega$ model	Vertical tube	2D	Ornatsky et al. [140]	-
Shen et al. [46]	FLUENT	SST $k-\omega$ model	Vertical tube	3D	Ackerman [82], Shen et al. [46]	-
Zhu et al. [141, 142]	CFX	RNG $k-\varepsilon$ , SST $k-\omega$ , Reynolds stress models of SSG, LRR and RSO	Vertical sub-channels	3D	Yamagata et al. [19]	SSG Reynolds stress model

ACCEPTED MANUSCRIPT

Table 5

Authors	CFD code	Assessed turbulence model	Flow geometry	Dimension	Benchmark data	Recommended turbulence model
Palko and Anglart [104, 107]	CFX 11.0	Standard $k-\varepsilon$ model, SST $k-\omega$ model	Vertical tubes	Unstated	Shitsman [22], Ornatskij et al. [130]	SST $k-\omega$ model
Sharabi and Ambrosini [153]	THEMAT (in-house code)	Standard $k-\varepsilon$ model, Low- $Re$ models of JL, LS, LB, CH, YS and AKN, $k-\omega$ model, $k-\tau$ model, SST $k-\omega$ model	Vertical tubes	2D	Yamagata et al. [19], Kim et al. [155]	-
Kao et al. [147]	FLUENT	RNG $k-\varepsilon$ model, Reynolds stress model (RSM)	Vertical tubes	2D	Yamagata et al. [19], Shitsman [22]	Reynolds stress model (RSM)
Wen and Gu [156]	FLUENT	Low- $Re$ $k-\varepsilon$ models of AKN, YS, CHC, AB, V2F; SST $k-\omega$ model	Vertical tubes	2D	Pis'menny et al. [30], Shitsman [22]	V2F model and SST $k-\omega$ model
Mohseni and Bazargan [109]	In-house code	Low- $Re$ $k-\varepsilon$ models of JL, LS, CH, MK, AKN and CK	Vertical and horizontal tubes	2D	Bazargan et al. [27], Song et al. [79]	Low- $Re$ $k-\varepsilon$ models of MK
Wen and Gu [108]	FLUENT	Low- $Re$ $k-\varepsilon$ models of AKN, YS, CHC, AB, V2F; SST $k-\omega$ model	Vertical tube	2D	Ornatskij et al. [130]	SST $k-\omega$ model
Bazargan and Mohseni [148]	In-house code	Zero-equation algebraic models of VD and BR, Low- $Re$ $k-\varepsilon$ models of MK and CK, $k-\omega$ model	Vertical tubes and annulus	2D	Yamagata et al. [19], Bae and Kim [157], Kim et al. [155]	-
Zhang et al. [106]	In-house code	Low- $Re$ $k-\varepsilon$ models of YS, AB, CH, AKN and LS, SST $k-\omega$ model, an	Vertical tube	2D	Zhang et al. [106]	The improved $k-\varepsilon-k_r-\varepsilon_r$ model

		improved $k-\varepsilon-k_t-\varepsilon_t$ model			
Jaromin and Anglart [158]	CFX 12.1	SST $k-\omega$ model	Vertical tubes	2D	Shitsman [22], Ornatskij et al. [130]
Kiss and Aszódi [150]	CFX 13.0	SST $k-\omega$ model	Vertical tube	3D	Shitsman [22], Ornatskij et al. [130]
Lei et al. [159]	FLUENT	Standard $k-\varepsilon$ model, RNG $k-\varepsilon$ model, SST $k-\omega$ model	Horizontal tube	3D	Yamagata et al. [19], Yu et al. [160]
Liu et al. [89, 161]	FLUENT	Low- $Re$ models of AB, LB, LS, YS, AKN, CHC and V2F, SST $k-\omega$ model	Vertical tubes and annulus	2D	Shitsman [22], Ornatskij et al. [130], Glushchenko and Gandziuk [162]
Wang et al. [77]	CFX	RNG $k-\varepsilon$ model, SST $k-\omega$ model, SSG Reynolds stress model	Vertical annuli	3D	Yang et al [63], Wang et al. [77]

Table 6

Authors	Assessed or proposed correlation	Benchmark data
Bazargan and Fraser [169]	$Pr_t = 1.855 - \tanh[0.2(y^+ - 7.5)]$	Bazargan and Fraser [169]
Mohseni and Bazargan [170]	$Pr_t = 0.75 + \frac{1.63}{\ln(1 + Pr/0.0015)}$ $Pr_t = 1.855 - \tanh[0.2(y^+ - 7.5)]$ $Pr_t = \begin{cases} 1.07 & y^+ \leq 10 \\ 2/Pe_t + 0.85 & y^+ > 10 \end{cases} \text{ in which } Pe_t = \frac{\mu_t}{\mu} Pr$ $Pr_t = \left\{ \frac{1}{7} + \frac{0.3Pe_t}{\sqrt{0.85}} - (0.3Pe_t)^2 \left[ 1 - \exp\left(-\frac{1}{\sqrt{0.85}(0.3Pe_t)}\right) \right] \right\}^{-1}$	Yamagata et al. [19] for water, Bae and Kim [157], Song et al. [79] and Bae et al. [84] for CO <sub>2</sub>
Mohseni and Bazargan [174]	$Pr_t(x, r) = Pr_{t,cr} \left[ 1 - \left( 1 - \frac{0.9}{Pr_{t,cr}} \right) \left( 1 - \frac{\beta(x,r)}{\beta_{max}} \right) \right]$ where $Pr_{t,cr} = -1.067X + 0.9$ , and $X = \left( \frac{P_{cr}}{P_{cr,CO_2}} \frac{P_{ref}}{P} \right) \left( \frac{M}{M_{ref}} \right) \left( \frac{d}{d_{ref}} \right)^{0.3} \frac{q}{G^2}$	Yamagata et al. [19], Song et al. [79] and Kim et al. [155] for CO <sub>2</sub>
Bae [171]	$Pr_t = 0.9 - f_1 f_2 (0.9 - Pr_{t,0})$ where $f_1 = 1 - \exp\left(-\frac{y^+}{A^+}\right)$ and $f_2 = 0.5 \left[ 1 + \tanh\left(\frac{B - y^+}{10}\right) \right]$	Shitsman [22] and Vikhrev et al. [93] for water, Bae [175] CO <sub>2</sub> , Mori et al. [176] for R22
Tian et al. [172]	$Pr_t = \begin{cases} 1.0 & y^+ \leq 5 \\ a + b \frac{Pr^2}{Pe_t} & 5 < y^+ < 100 \\ 0.85 & 100 \leq y^+ \end{cases} \text{ where } Pe_t = \frac{\mu_t}{\mu} Pr$	Gu et al. [43] for water, Zahlan et al. [177] for CO <sub>2</sub> , Feuerstein et al. [178] for R134a

Table 7

References	Correlations	Flow Geometry	Applicability Range
Cheng et al. [42]	$Nu_b = 0.023Re_b^{0.8}Pr_b^{0.33}F, \text{ where } F = \min(F_1, F_2)$ $F_1 = 0.85 + 0.766(\pi_A \cdot 10^3)^{2.4}$ $F_2 = \frac{0.48}{(\pi_{A,pc} \cdot 10^3)^{1.55}} + 1.21 \left(1 - \frac{\pi_A}{\pi_{A,pc}}\right) \text{ and } \pi_A = \frac{\beta_b q}{G c_p}$	Tubes ( $D=10, 20$ mm)	$P=22.5-25$ MPa; $G=700-3500$ kg/m <sup>2</sup> s; $q=300-2000$ kW/m <sup>2</sup> ; $t_b=300-450$ °C
Gupta et al. [18]	$Nu_w = 0.004Re_w^{0.923}\overline{Pr}_w^{-0.773} \left(\frac{\mu_w}{\mu_b}\right)^{0.366} \left(\frac{\rho_w}{\rho_b}\right)^{0.186}$	Tube ( $D=10$ mm)	$P=24$ MPa; $G=200-1500$ kg/m <sup>2</sup> s; $q=70-1250$ kW/m <sup>2</sup> ; $t_{in}=320-350$ °C
Mokry et al. [35]	$Nu_b = 0.0061Re_b^{0.904}\overline{Pr}_b^{-0.684} \left(\frac{\rho_w}{\rho_b}\right)^{0.564}$	Tube ( $D=10$ mm)	$P=24$ MPa; $G=200-1500$ kg/m <sup>2</sup> s; $q=70-1250$ kW/m <sup>2</sup> ; $t_{in}=320-350$ °C
Liu and Kuang [193]	$Nu_b = 0.01Re_b^{0.889}\overline{Pr}_b^{-0.730} \left(\frac{\lambda_w}{\lambda_b}\right)^{0.240} \left(\frac{\mu_w}{\mu_b}\right)^{0.153} \left(\frac{\rho_w}{\rho_b}\right)^{0.401} \left(\frac{\bar{c}_p}{c_{pb}}\right)^{0.014} Gr^{*0.007} \left(\frac{q\beta_b}{Gc_{pb}}\right)^{0.041}$	Tubes ( $D=6-38$ mm)	$P=22.4-31$ MPa; $G=200-3500$ kg/m <sup>2</sup> s; $q=37-2000$ kW/m <sup>2</sup> ; $H_b=93-3176$ kJ/kg
Chen and Fang [194]	$Nu_b = 0.46Re_b^{0.16} \left(\frac{Pr_w}{Pr_b}\right)^{0.1} \left(\frac{\nu_w}{\nu_b}\right)^{-0.55} \left(\frac{\bar{c}_p}{c_{pb}}\right)^{0.88} \left(\frac{Gr_b^*}{Gr_b}\right)^{0.81}$	Tubes ( $D=6-26$ mm)	$P=22-34.3$ MPa; $G=201-2500$ kg/m <sup>2</sup> s; $q=129-1735$ kW/m <sup>2</sup> ; $H_b=278-3169$ kJ/kg
Deev et al. [101]	$Nu_b = 0.026Re_b^{0.8}Pr_b^{0.4} \left(\frac{\rho_w}{\rho_b}\right)^{0.25} \left(\frac{\bar{c}_p}{c_{p,b}}\right)^n \varepsilon(B_m) \text{ where } B_m = \frac{q}{G H_{pc}-H_b }$	Annuli (gap of 2.67-6 mm), 2×2 bundles ( $D_{hy}=2.4-5.4$ mm)	$P=22.6-28$ MPa; $G=350-2700$ kg/m <sup>2</sup> s; $q=200-3200$ kW/m <sup>2</sup> ; $H_b=865-3144$ kJ/kg

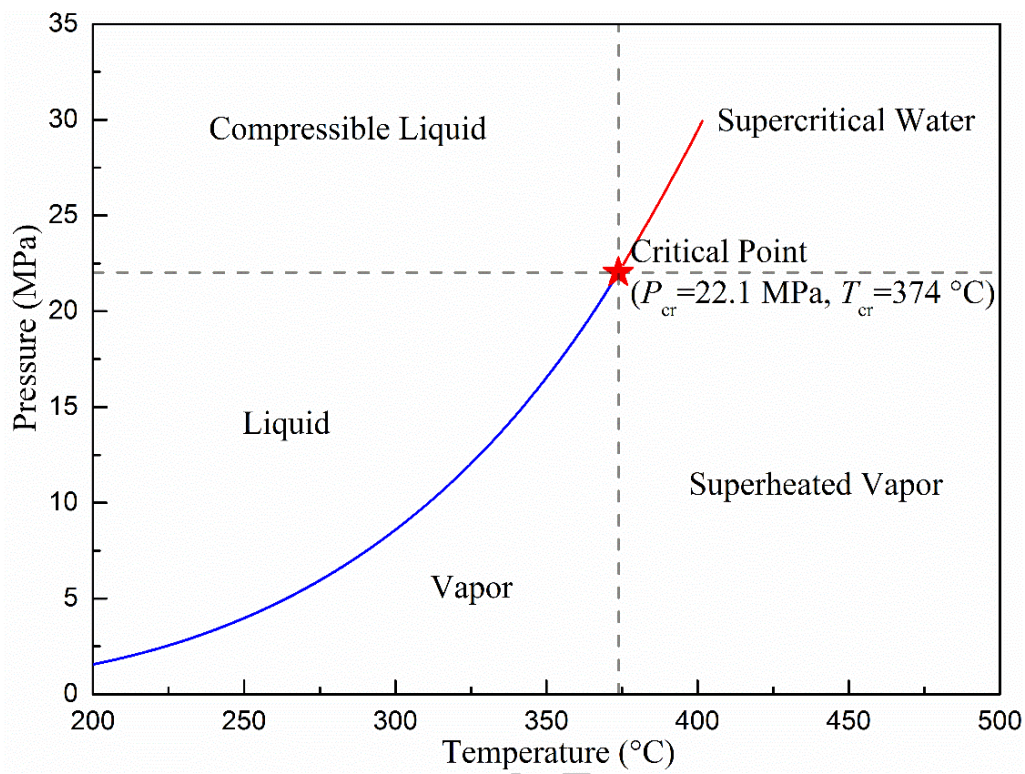


Figure 1

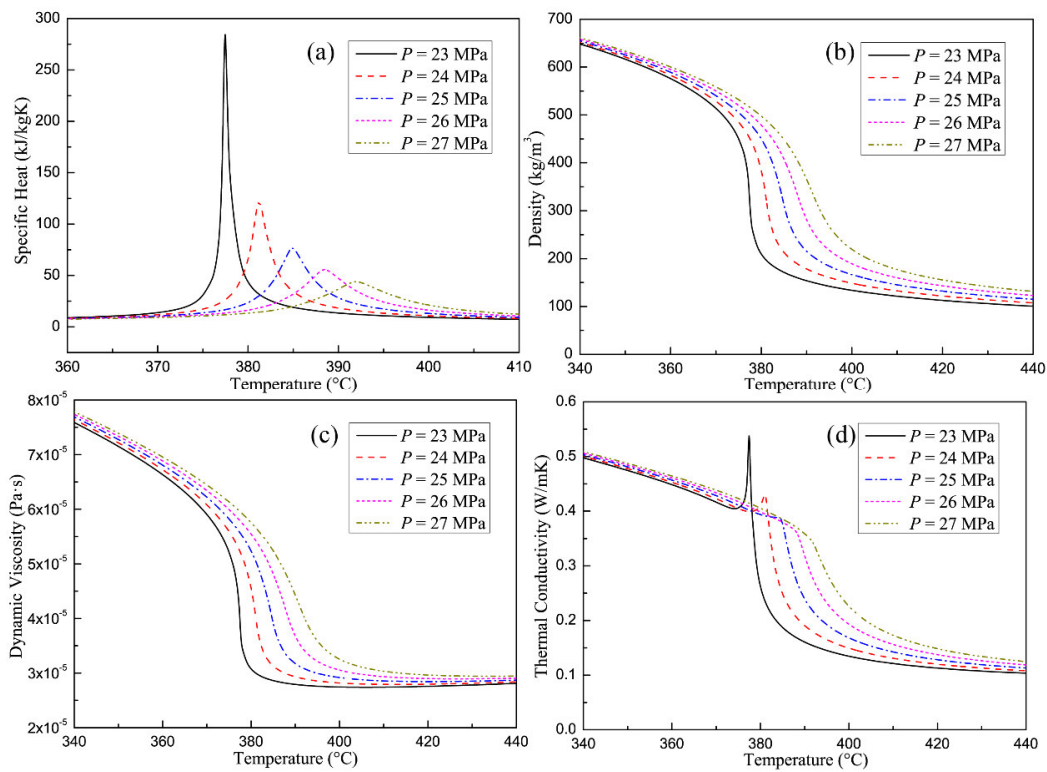


Figure 2

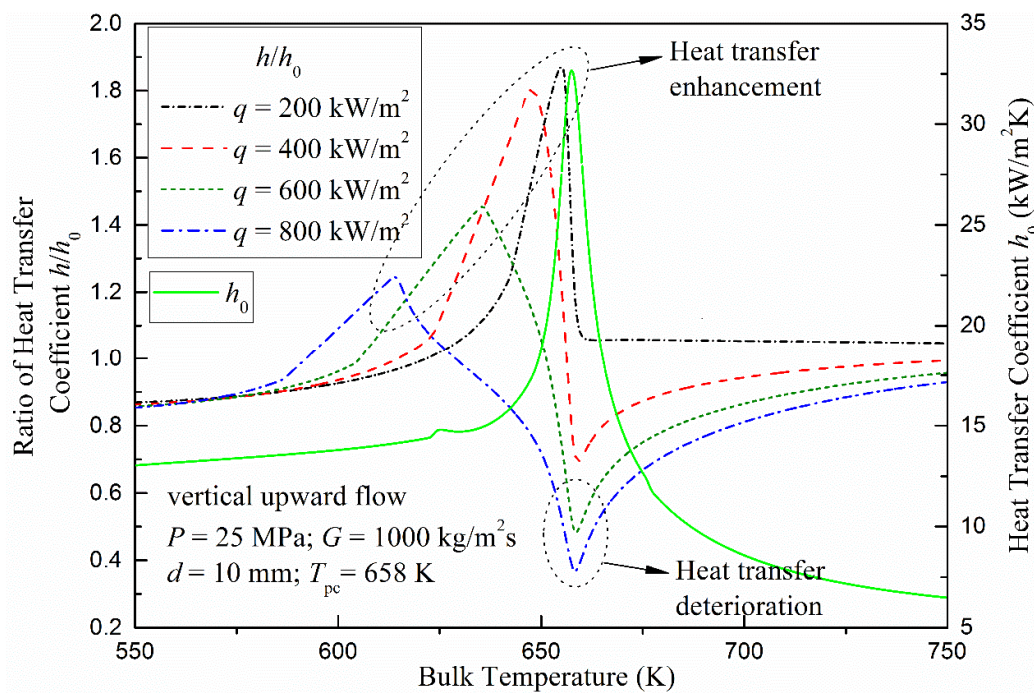
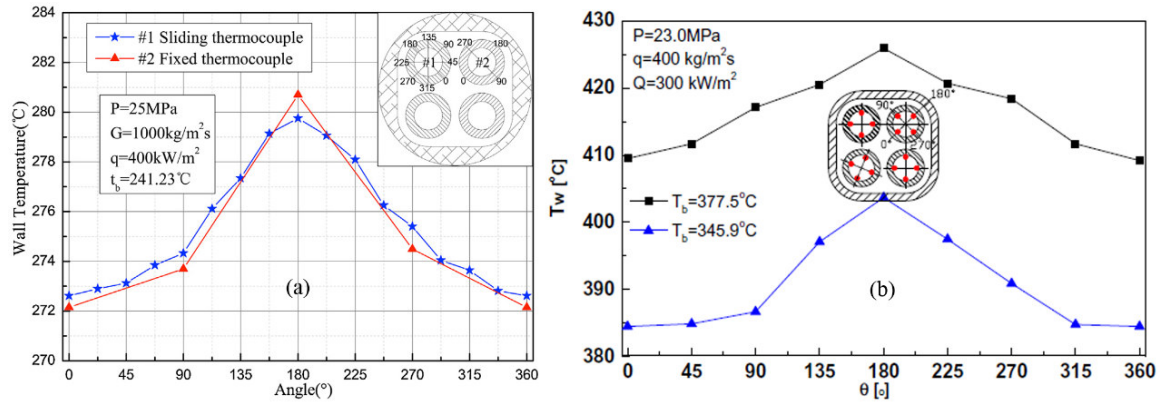


Figure 3



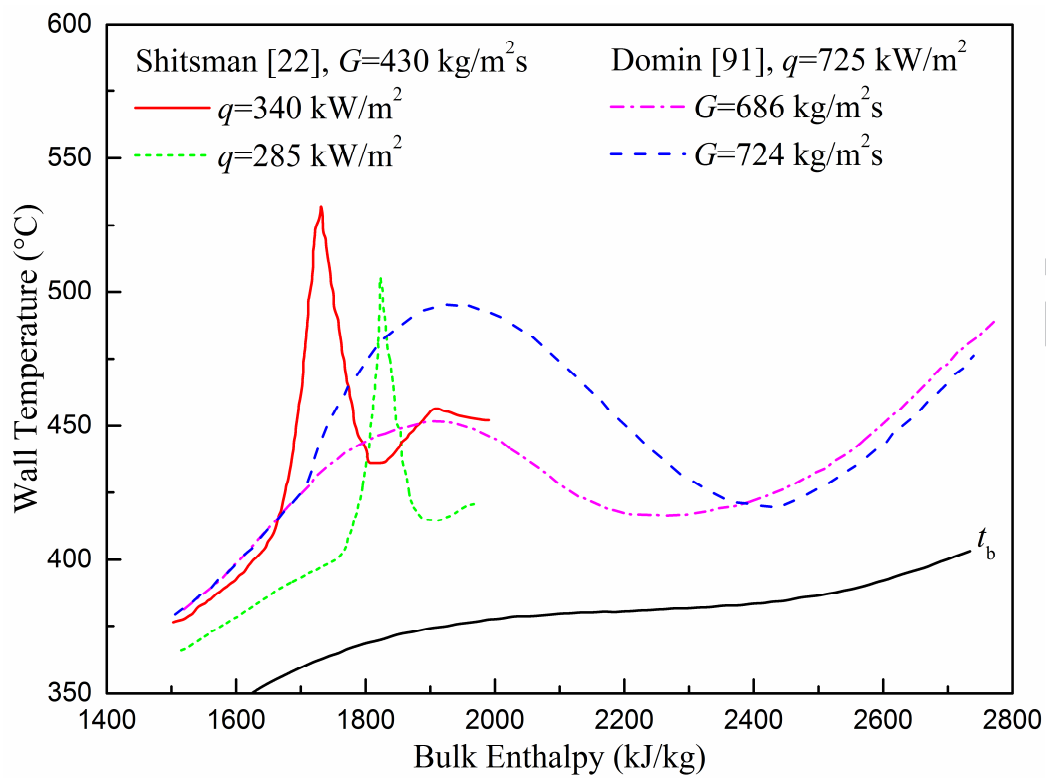


Figure 5

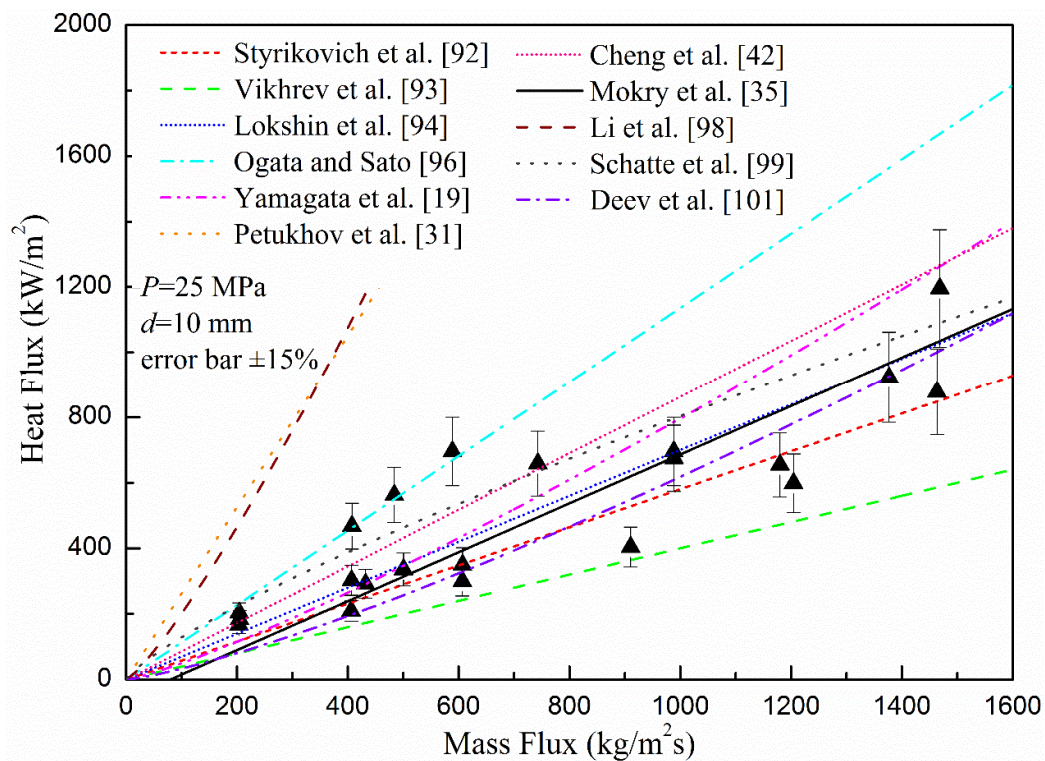


Figure 6

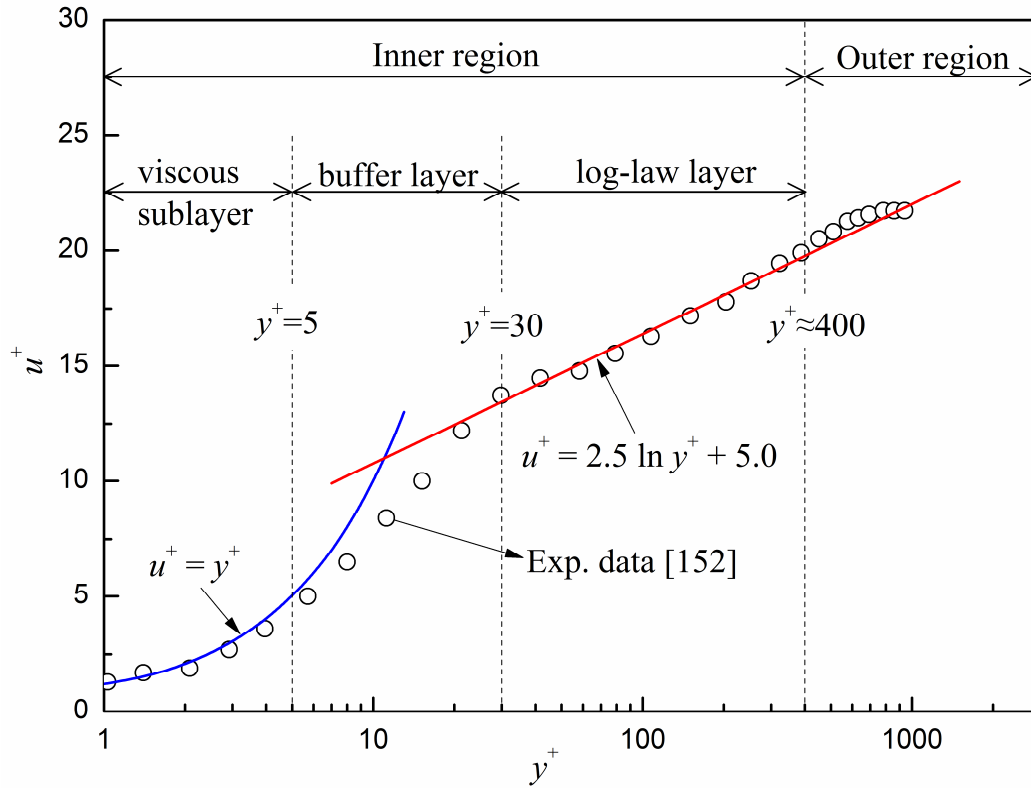


Figure 7

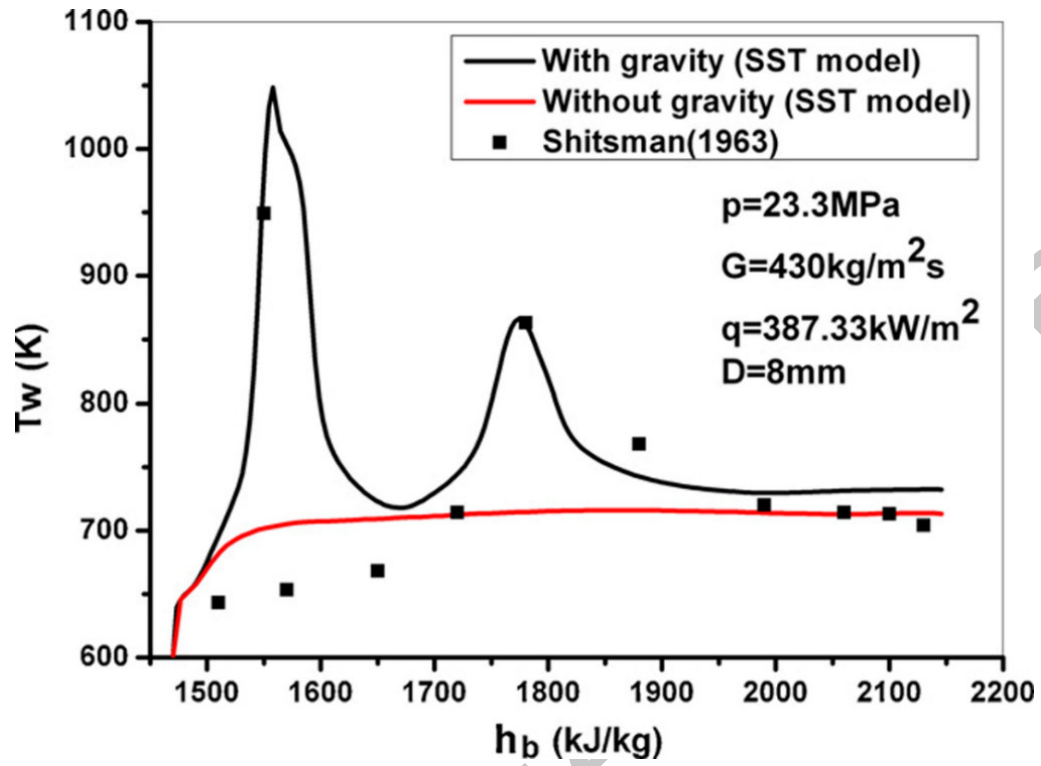


Figure 8

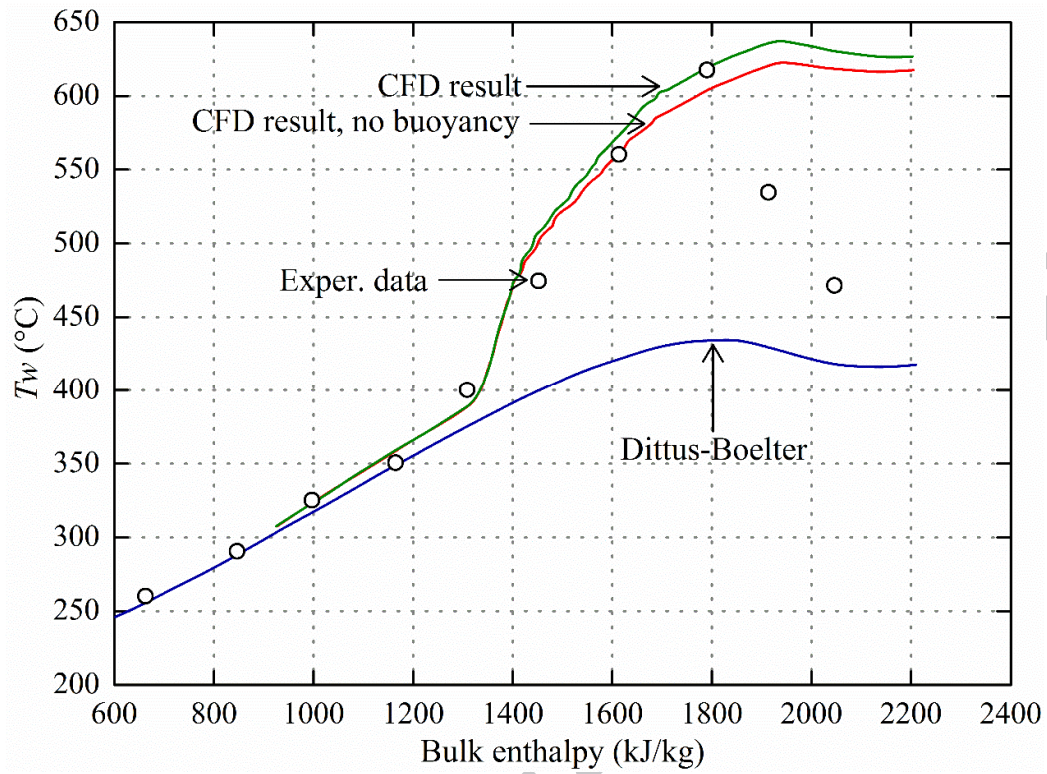


Figure 9

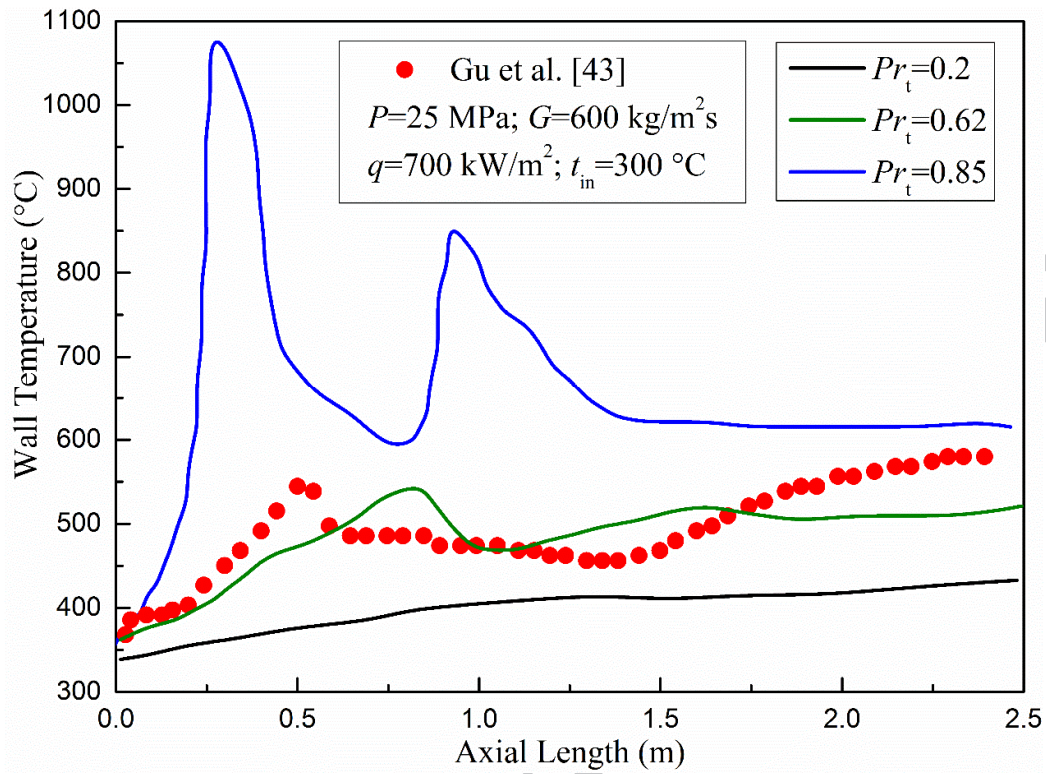


Figure 10

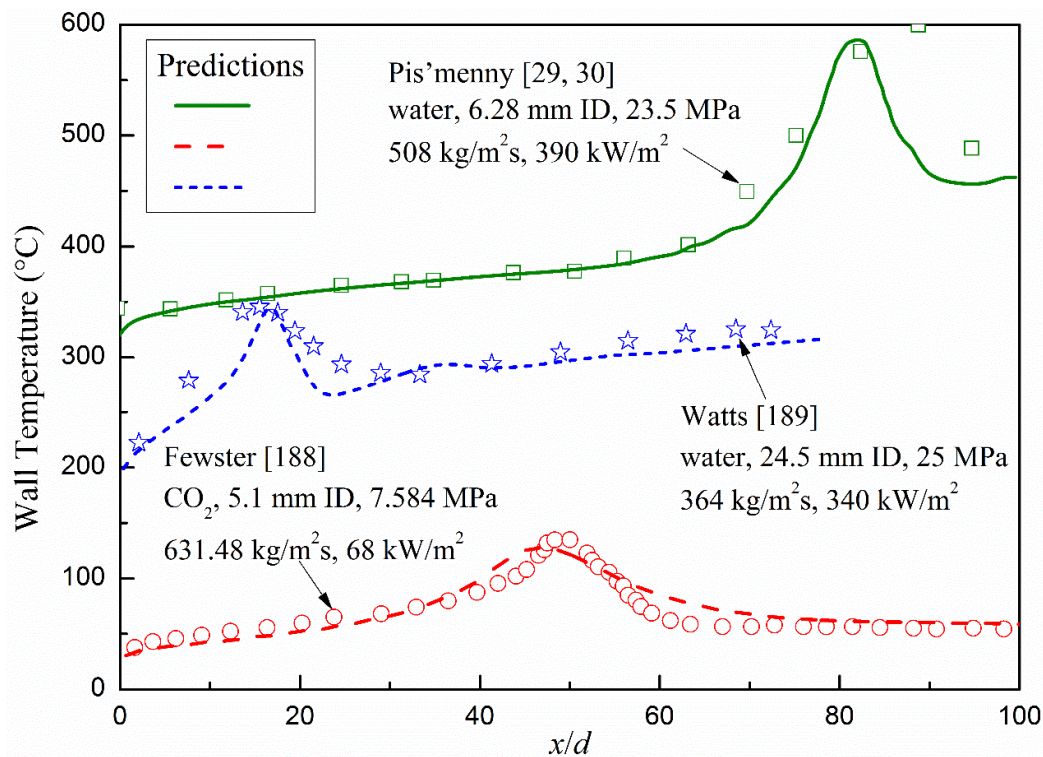


Figure 11

### Highlights

- Experimental and numerical studies of heat transfer to SCW were reviewed.
- The effects of several factors on heat transfer were discussed.
- Deteriorated heat transfer were summarized and analyzed.
- The validation of various turbulence models was studied.
- Suggestions were provided in developing new prediction correlations.